IEEE Access
Multidisciplinary | Rapid Review | Open Access Journal

Received 21 May 2023, accepted 20 June 2023, date of publication 21 July 2023, date of current version 14 August 2023.

Digital Object Identifier 10.1109/ACCESS.2023.3297982

RESEARCH ARTICLE

Handover Reduction in 5G High-Speed Network Using ML-Assisted User-Centric Channel Allocation

MOSTAFA RAEISI AND ABU B. SESAY, (Life Senior Member, IEEE)
Department of Electrical and Software Engineering, University of Calgary, Calgary, AB T2N 1N4, Canada

Corresponding author: Mostafa Raeisi (mostafa.raeisiziaran@ucalgary.ca)

This work was supported in part by the Natural Sciences and Engineering Research Council of Canada, and in part by the Schulich School of Engineering, University of Calgary.

ABSTRACT In this paper, we propose a novel user-centric channel allocation scheme for high-speed terrestrial users of the Fifth Generation (5G) network in the millimetre-Wave (mm-Wave) band small-cells named Vehicular Frequency Reuse (VFR) scheme. To adapt the VFR scheme with the 5G network, we develop a new mobility management function that improves the 5G's performance for high-speed road users such as Connected Autonomous Vehicles (CAV) in small-cells by reducing the number of handovers (HOs) in the Vehicle-to-Network (V2N) service. The VFR scheme significantly reduces the users' HO rate, control plane signalling in air interface, and improves link reliability and channel reuse ratio. A metric called Distance-Threshold (DT) is defined to determine the frequency reuse ratio for the 5G network with the VFR scheme. We also propose a new cell reselection procedure for high-speed users in RRC_Connected (Radio Resource Control) state that are using the VFR scheme and managed by our mobility management function. The proposed cell reselection procedure is defined for inter-gNB-DU (gNodeB-Distributed Unit) and intra-gNB-DU mobility. This procedure reduces traffic load on the UE's (User Equipment) air interface, lowers processing and signalling load for network nodes, and assists for seamless mobility management for high-speed users. These all help and facilitate the path towards the targeted zero millisecond mobility interruption time (MIT) for 5G-NR (New Radio) users. Moreover, the proposed scheme, function, and procedure are compatible with the existing 5G structure and user equipment and can be easily added to the network by only software patches. The proposed mobility management function separates low-speed and high-speed users to serve them accordingly with different sets of channels. To separate high-speed and low-speed users, we propose a simple scalar metric defined as a Velocity-Threshold (VT). The VT value is adaptively calculated by a K-Means approach which is a well known unsupervised Machine Learning (ML) algorithm, according to the road condition inferred from reported velocities. Finally, we evaluate the proposed VFR scheme and compare it with the traditional cell-centric channel allocation scheme. Computer simulations show that the proposed VFR scheme can reduce the number of HOs (HO rate) for users by over 99% compared with the traditional scheme.

INDEX TERMS 5G, autonomous vehicle, channel allocation, connected vehicles, frequency planning, high-mobility, high-speed, K-means, mobility control, mobility management.

I. INTRODUCTION

In the transportation industry, a general definition of an autonomous system is a system that can sense, measure, plan, control, adapt to its environment, and perform a task with little or no human intervention [1]. The term autonomous has recently been used in areas such as unmanned aircraft systems, autonomous ships, autonomous robots, autonomous drones, and Autonomous Vehicles (AVs). The concept of AV started in the 1920s and was referred to as phantom autos, which were remote-controlled by tapping on the telegraph key that needed someone to follow the car to control it. During

The associate editor coordinating the review of this manuscript and approving it for publication was Mauro Tucci.

the last decade, the concept of AVs has become very different and now we expect vehicles to sense their environment and drive without human intervention or with little control.

Driving is a complicated task that humans can easily cope with while for computers, it is a complicated function and needs lots of hardware and software resources. AVs need various sensors and measuring equipment such as cameras, radars, lidars, ultrasonics, sonars, localization and navigation systems, and Inertial Navigation Systems (INS). The dynamics of the surrounding environments of an AV enforce real-time processing of these sensors' data. Furthermore, processing intensity depends on traffic jams, weather conditions, road situation, time of day, and many other parameters. Processing all these data and implementing related algorithms need fast processors to support the peak processing time. These continuous heavy-duty processing increase the hardware cost and sink valuable limited battery power in AVs. To solve this issue, AVs can use distributed processing resources outside the vehicle. The AVs access these resources through wireless communication links whenever available and needed.

AVs with ability to communicate with surrounding devices, vehicles, and infrastructure to gain access to more resources are known as Connected Autonomous Vehicles (CAV). The resources include hardware, applications, services, and data. Communications in AVs are in two general forms Intra-Vehicle and Inter-Vehicle communications. Intra-Vehicle communication includes any wired or wireless link between the devices in a vehicle. This type of communication uses various technologies such as Controller Area Network (CAN), Ethernet, Low-Voltage Differential Signalling (LVDS), and some others for wired links and Bluetooth, ZigBee, Ultra-Wideband (UWB), and Wi-Fi for wireless transmissions.

Inter-Vehicle communication is an interaction between AV and other vehicles or devices via wireless links. It uses Bluetooth and ZigBee wireless technology standards for low power communications, Wi-Fi, and Dedicated Short-Range Communications (DSRC) for IEEE based links, WiMAX, Long Term Evolution-Vehicle (LTE-V), and 5G (the Fifth Generation) for base station driven connections and Heterogeneous Vehicular Network (HetVNET), Software-Defined Networking (SDN), and Visible Light Communication (VLC) for auxiliary transmissions [9], [10], [11].

Inter-Vehicle communication includes Vehicle-to-Cloud (V2C), Vehicle-to-Grid (V2G), Vehicle-to-Pedestrian (V2P), Vehicle-to-Vehicle (V2V), Vehicle-to-Infrastructure (V2I), and Vehicle-to-Network (V2N). In general, Vehicle-to-Everything (V2X) communication represents all the inter-vehicle communications. The V2X communication was listed in Release 14 for vehicular network by the 3rd Generation Partnership Project (3GPP). V2X communication is the exchange of information between a vehicle and any entity connected to the vehicle. Using V2X communication, vehicles can benefit from distributed edge computing and storage resources, gain access to the closest control services on the network edge, and communicate with other vehicles in the vicinity. Moreover, a vehicle can gain access to several non-safety Internet services such as web browsing, video streaming, file downloading, high-quality map, online gaming, and other infotainment services [2], [3], [4]. Use cases and applications of V2X were put in four groups vehicle platooning, advanced driving, extended sensors, and remote driving according to [5].

V2N communication is the gateway for CAVs' access to the Internet, road side processing resources, safety and infotainment data, and in general connect to the world beyond their immediate vicinity. One of the most suitable and feasible technologies for these communications is the 5G network. 5G's radio access technology developed by the 3GPP is called 5G-NR (New Radio). 5G-NR's design targeted to fulfill a set of features that are crucial for future vehicular networks including fast-moving vehicles and High-Speed Trains (HSTs) with a speed of up to 500 km/h [6], [7]. The goals include low latency, high data rate and capacity (up to 20 Gbps for peak data rates and 100 Mbps wherever needed), enormous number of users (up to 100x of LTE network), ultra-high reliability (99.999% and beyond), lower energy usage, less service cost, and more coverage in comparison with previous generations [8], [9], [10].

To achieve these goals, 5G will use more frequency bands, including sub-6 GHz and millimetre-Wave (mm-Wave) bands, compared to LTE (Long Term Evolution). Furthermore, 5G has the advantage of beam-forming, large antenna arrays, spatial multiplexing, cell densification, shared spectrum, device-centric architecture, and Device-to-Device (D2D) communications concepts [9], [10].

New technologies added to 5G include multi-user Multiple Input Multiple Output (MIMO), massive-MIMO, smart-antenna, Non-Orthogonal Multiple Access (NOMA), full-duplex communication, flexible and powerful nodes at the edge, mobile edge computing, optimized content delivery, device-centric architecture, mm-Wave, Cloud Radio Access Network (RAN), SDN, and Network Function Virtualization (NFV) [8], [9], [10], [11]. Most of these technologies are critical for CAVs to drive safely and reliably on roads. Therefore, only 5G and following generations such as 6G (Sixth Generation) are viable wireless technologies for safe autonomous vehicles in future [8], [9], [10], [11].

5G uses advanced small-cells, moving back-haul, fast and seamless Handover (HO), and fully distributed network to satisfy the unprecedented low latency and high data rate [12]. In addition, 5G considered some special configurations for high speed scenarios to support users with speeds of up to 500 km/h as specified in [13] and [14]. 5G small cells include femtocells and picocells with cell radius down to a few meters. The combination of a large number of users and the application of femtocells or picocells increases the number of HOs by at least two orders of magnitude [9]. Moreover, traffic of high-speed users such as CAVs and HSTs through the small-cells require frequent HOs between cells every few seconds. Frequent inter-cell mobilities and HOs, add a lot of controlling traffic (RRC messages) to wireless control channels that not only waste valuable wireless resources, but also increase the chance of connection loss and drop in Quality of Experience (QoE).

The traditional channel allocation scheme was designed based on users random movement in arbitrary directions that is suitable for pedestrian users. A pedestrian might change their path at any moment and could walk in any direction. Moreover, human walking speed is considerably slower than a high-speed vehicle or a train. Therefore, for a pedestrian in past generations cells (base stations) with a few kilometre coverage area, relocating from a cell to another was taking a long time. Also, the transition time in two cells overlap area (the region covered by two neighbour cells that helps for successful HO) was big enough for the network to successfully establish a HO. In addition to the above points, considering the lower number of users, less data rate demand, and less strict Quality of Service (QoS) requirements made the traditional cell-centric channel allocation scheme a sufficient solution at the time. However, for 5G and beyond with ten times increase in the number of users with the addition of small-cells and high-speed user, providing the promised high data rate and QoE with the legacy radio resource management scheme could be very challenging.

The incentive of our scheme is the predictable and predetermined moving path of vehicles on a road and also vehicles homogeneous driving speed in each direction of a road, particularly in future autonomous vehicles. However, we are aware of the intersections, U-turns, and other road variables and the proposed plan covers all of them. These two main characteristics of high-speed road users can be used by the cellular network to have an estimate of user's entry to a new cell and be ready in advance for the next cell of these users. Also, their relative distance to each other permits the use of one channel for two vehicles only a few hundred meters apart while they are located in separate small-cells with at least one cell in between.

The key contributions of this paper include proposal of a new Mobility Management Function (MMF) for the 5G Radio Resource Control (RRC) and a novel channel allocation scheme for high-speed users (such as CAVs) connected to the 5G network without any hardware or structural change in the 5G. The proposed channel allocation is a vehicle-oriented scheme for high-speed users that can coexist with 5G's cell-oriented channel allocation in the same infrastructure which reduces the number of HOs for CAVs and other high mobility cellular users. The main contribution of this paper includes:

- A new mobility management function for 5G RRC to control the mobility of both high-speed and low-speed users with two different procedures to reduce the number of HOs in the network. The new function separates users by only relying on their speed and comparing it with a metric.
- A novel Vehicular Frequency Reuse (VFR) scheme for V2N link between high-speed vehicles and small-cells. The proposed VFR scheme is a user-centric channel allocation method that assigns a channel to a high-speed vehicle from a separate list than the users in the conventional cell-centric scheme. The assigned channel stays with the vehicle as it traverses multiple cells. The VFR scheme reduces the number of HOs for users considerably; which improves the network performance, control plane efficiency and link reliability.
- A novel cell reselection procedure for high-speed users in RRC_Connected state is proposed to manage their relocation between cells. This procedure helps the network to direct the user data traffic to the cell that it is currently located in. This procedure is almost invisible in the user's perspective and the user just needs to be informed about its serving cell ID (Cell Identifier) for following measurement reports.
- Investigation of the frequency reuse ratio in the proposed method. We formulate the minimum distance between two CAVs that can use the same channel according to the applied antennas on each side of the user and the network that is called Distance-Threshold.
- To reduce co-channel interference and avoid unnecessary HOs for pedestrians and vehicles, we separate low-speed and high-speed users by their reported speeds using a proposed Velocity-Threshold (VT) metric. We investigate the VT calculation using a Machine Learning (ML) algorithm adaptively, according to the road and environment conditions.
- A study of traditional channel allocation schemes, measurement reports, and HO procedure in the 5G network.

The rest of the paper is organized as follows. In Section II, a brief background of the architecture and HO procedure in the 5G network is provided. In Section III, related literature is studied and compared with the proposed method. Our system model is presented in Section IV. The proposed mobility management function in comparison with the conventional MMF is provided in Section V. Section VI includes the proposed VFR cell reselection procedure. The proposed VFR channel allocation scheme is described in Section VII. The proposed Distance-Threshold (DT) metric is calculated and evaluated in Section VIII. Section IX presents the Velocity-Threshold (VT) metric for the proposed MMF. A comparison between our VFR scheme's performance and traditional channel allocation scheme for high-speed users is provided in Section X. Finally, we provide a conclusion in Section XI. A list of the frequently used abbreviations throughout this paper is provided in an Appendix for ease of access.

II. BACKGROUND

In this section, we provide the background information for the 5G network based on 3GPP's documents and recent literature.

A. 5G NETWORK ARCHITECTURE

The Architecture of the 5G cellular network can be split into the core network and a RAN as shown in Figure 1. The RAN of 5G is referred to as the Next Generation-RAN

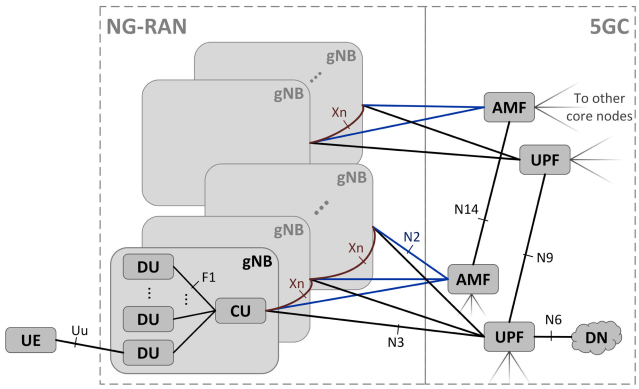

FIGURE 1. The 5G network architecture based on 3GPP model.

(or NG-RAN) as in Figure 1. The NG-RAN consists of several nodes labelled as gNodeB (or gNB). A gNodeB provides user-plane and control-plane protocol terminations towards the User Equipment (UE). A gNodeB is connected to the 5G Core (5GC) either directly or indirectly. The direct connection is through NG interfaces while the indirect connection is through other gNodeBs. The indirect connection is also known as Integrated Access and Backhaul donor (IAB-donor) [15]. The 3GPP splits the gNodeB functions into two units, namely the Central Unit (CU or gNB-CU) and the Distributed Unit (DU or gNB-DU).

The ITU Telecommunication standardization sector (ITU-T), on the other hand, considers a third unit called the Radio Unit (RU) in addition to the CU and DU in the 3GPP [16], [17]. A gNodeB with functions split between gNB-CU and gNB-DU (and RU if applicable) is referred to as a split-cell model. In the ITU-T model, the RU mostly handles the Radio Frequency (RF) function of the gNodeB and is responsible for the wireless link between the network and the users. The RU unit might also include the low- and high-Physical functions in addition to the RF function [17]. In the 3GPP model, the DU can be considered as a combination of the DU and RU units in the ITU-T model.

In the 3GPP's NG-RAN architecture, there are different functional split options between CU and DU [18]. The most common functional split is where the gNB-CU hosts the RRC, the Service Data Adaptation Protocol (SDAP), and the Packet Data Convergence Protocol (PDCP), while the gNB-DU hosts the Radio Link Control (RLC), Medium Access Control (MAC), and Physical (PHY) layers [16]. Each gNodeB has only one gNB-CU that can be divided into two logical nodes, the gNB-CU-Control Plane (gNB-CU-CP) and gNB-CU-User Plane (gNB-CU-UP). Each gNB-CU controls the operation of one or multiple gNB-DUs as shown in Figure 1 [16]. Each gNB-DU can support one or more cells.

In the 3GPP specifications, there are two operating Frequency Ranges (FR), FR1 and FR2 (for 5G-NR) [6]. The frequency range FR1 covers the range 410 MHz to 7125 MHz (below 6 GHz), while the FR2 covers mm-Wave frequency band, above 24 GHz in two sub-ranges FR2-1 (24250 MHz - 52600 MHz) and FR2-2 (52600 MHz - 71000 MHz). The mm-Wave frequencies provide wide bandwidths and high data rates, but at the cost of high power transmission loss, poor diffraction rate, and high sensitivity to obstacles. Therefore, the mm-Wave bands are more suitable for small-cells such as micro-cells, pico-cells, or femto-cells where Line-of-Sight (LOS) transmission is beneficial. On the other hand, such small cells result in increased numbers of users traversing several cells, which in turn can significantly increase the numbers of HO requests.

B. SMALL-CELLS AND RSUs

Small-cells have the advantage of increasing the frequency reuse ratio. Also, they do not need massive antenna towers with dedicated land for equipment installation which can limit base station installation locations and increase Capital Expenditure (CAPEX) for operators. Therefore, small-cells help to provide high data-rate, coverage, and reliability demands of 5G users at low power consumption and service cost for both indoor and outdoor areas.

Based on 3GPP's definition, a Road-Side Unit (RSU) is a logical entity that provides V2X communication for users using either gNodeB or UE-provided functionality [19]. Accordingly and for simplicity, in this paper, the RSU refers to a 5G small-cell that is installed alongside the road to provide cellular (V2N) communication for road users such as vehicles or pedestrians. In terms of deployment, a RSU is different than a gNodeB and might be deployed by road authorities as well as network operators [5].

For better cellular coverage of roads and cost reduction of network development, RSUs can be installed in lampposts with Inter-Site Distance (ISD) in a few tens of meters up to a few hundreds of meters to service high-speed users [20], [21].

C. HANDOVER IN 5G-NR

Handover, also known as handoff, is the procedure of changing the Primary Cell (PCell) of an ongoing session to another cell [14]. The HO might be required because of numerous changes in the network, namely a user relocation from a cell to another or a sector of a cell to another, weak received signal quality, load balancing between cells, or some other reasons.

In cellular networks, each cell (or a sector of a cell) is assigned with a portion of all available channels and to avoid interference, each cell's assigned channels are different than its neighbour cells. Therefore, each time a user approaches the edge of a cell to enter a new cell, the HO process is triggered as the user's channel is not valid in the new cell. Therefore, in 5G small-cells with high mobility users like CAVs and HSTs, the number of HOs will be considerably higher than a network with macro-cells.

The HO procedure consists of a series of messages (ranging between 12 to 19 steps) between a UE and 5G components such as gNB-DU, gNB-CU, and some of the 5GC components [16]. So, it consumes network processing and wireless link resources and could negatively affect users' QoE. To illuminate the effect of small-cells in a 5G-connected vehicular network, consider a vehicle with a speed of 120 Km/h driving through a network consisting of small-cells with a 100-meter diameter. In this case, the HO process is triggered every 3 seconds, and this trigger time will be even shorter at higher speeds, smaller cell coverage radii, or for a car passing through cell chords instead of the diameter.

In 5G the gNodeB is responsible for managing the HO and the decision happens in the gNB-CU-CP (Control plane of the gNodeB-CU unit). More specifically, the RRC protocol in gNB-CU manages the HO in each gNodeB. One of the main functions of the RRC protocol is the establishment, modification, suspension, resumption, or release of Radio Bearers (RBs) carrying user data (user-plane channels) [13].

RRC has three states, namely RRC_Connected, RRC_Inactive, and RRC_Idle. A UE resides in one of these states based on its network activity and RRC connection establishment. For a user, the state transition can happen from any state to another based on the user's network activity, except from RRC_Idle to RRC_Inactive. When a UE has no RRC connection to the 5G (e.g., UE's device is just switched on), it is in the RRC_Idle state. If the RRC connection is established between a UE and a gNodeB, it can be in one of the two states of RRC_Connected or RRC_Inactive. A UE is in the RRC_Connected state if it has a RRC connection and active data traffic with NG-RAN. Otherwise, if it just has a RRC connection, but no data traffic at the moment, the network puts it in the RRC_Inactive state. The HO procedure is only applicable in the RRC_Connected state for UE's mobility management such as HO to a new channel, or switch between Radio Access Technologies (RATs). In the RRC_Idle and RRC_Inactive states, cell selection and reselection processes are used to control the UE's mobility. A UE releases the assigned resources when it transits to the RRC_Idle state from any of the other two states and needs resource establishment when switching from RRC_Idle to RRC_Connected. This switching takes a long time compared with transitioning from RRC_Inactive to RRC_Connected. The RRC_Inactive state is a new state added to 5G as a state between the other two states to reduce transition time to RRC_Connected. Therefore, resources are suspended and resumed when UE transits between RRC_Inactive and RRC_Connected states (Subclause 4.2.1 of [13], [23]).

In the RRC_Connected state, the UE mobility is addressed by a HO procedure. There are multiple types of HOs with different signalling procedures depending on the source and target cell logical connection, as shown in Figure 2. It should be noted that during a HO procedure, the current cell is called the source or serving cell and the future cell is the target or candidate cell. In general, HO can be divided into two main types, inter-PLMN (Public Land Mobile Network) and intra-PLMN HOs. The inter-PLMN HO is required if the serving PLMN needs to be changed during the HO, in cases such as moving between countries, operators, or using a roaming service. Each of these two HOs is further divided into two types - inter-RAT and intra-RAT HOs [24]. The UE mobility from 5G to other RATs (or vise versa) is handled by inter-RAT HO procedure [13], [14]. To date, 22 RAT types are listed in 3GPP's technical specification for 5G networks (Subclause 8.17 of [25]). Some of these 22 RAT types include Universal Terrestrial Radio Access Network (UTRAN), GSM/EDGE Radio Access Network (GERAN), Wireless Local Area Network (WLAN), Evolved Universal Terrestrial Radio Access Network (EUTRAN).

The intra-RAT HO can be further divided into inter-AMF (Access and Mobility Management Function) and intra-AMF HOs. The inter-AMF HO, also known as N2 HO or N2 based HO in 3GPP documents, happens in cases where the source and target cells are in two different AMFs. In this case the Xn interface cannot be used for the HO procedure [24]-4.9.1.2.1. The intra-AMF HO is further divided into two types - inter-gNB-CU and intra-gNB-CU HOs. The inter-gNB-CU HO is handled by the gNB-CUs of the serving and target cells over the Xn interface (Figure 1). When both of the serving and target cells are managed by one gNB-CU, the intra-gNB-CU HO is required. The intra-gNB-CU has two types of inter-gNB-DU and intra-gNB-DU HOs. The intra-gNB-DU HO has two forms of inter-cell and intra-cell HO when there are multiple cells within one gNB-DU [16]. Lastly, the intra-frequency HO arises when the objective of the HO procedure is changing the UE's active channel within the same frequency range (in either FR1 or FR2 bands). The inter-frequency HO can happen in any of the following frequency range changes from FR1 to FR2, FR2 to FR1, FR1 to FR1, or FR2 to FR2 [14]-6.1.1.

Cellular users continuously measure their received signal quality from its serving cell and all the neighbouring cells and periodically report their condition to the serving cell's gNB-CU by a RRC measurement report message. The network might also set a UE to send an event report if a specific measurement exceeds a predefined threshold. Therefore, gNodeB constantly receives and monitors users' condition and take action accordingly. The cellular network finds about a user's transition between cells, when the serving cell's signal quality drops below a threshold and the target cell's signal level improves above another threshold. Accurate setting of these thresholds prevent unnecessary HOs and decrease chance of connection loss.

Decision about the time to start the HO and the type of the HO, is based on the UE's measurements of the received signal quality. The gNB-CU checks the UE's measurements from the serving and the neighbour cells included in the UE's report, to find the candidate cell(s) for HO. If there is an available channel in the candidate cell, the HO procedure is initiated. UE's signal quality measurements can be a Reference Signal Received Power (RSRP), Reference Signal Received Quality (RSRQ), Received Signal Strength Indicator (RSSI), Signal to Interference plus Noise Ratio (SINR), and some other measurement as specified in Subclause 5.5.3.1 of [13]. These measurements are with respect to the reference signals in the serving cell and neighbouring cells.

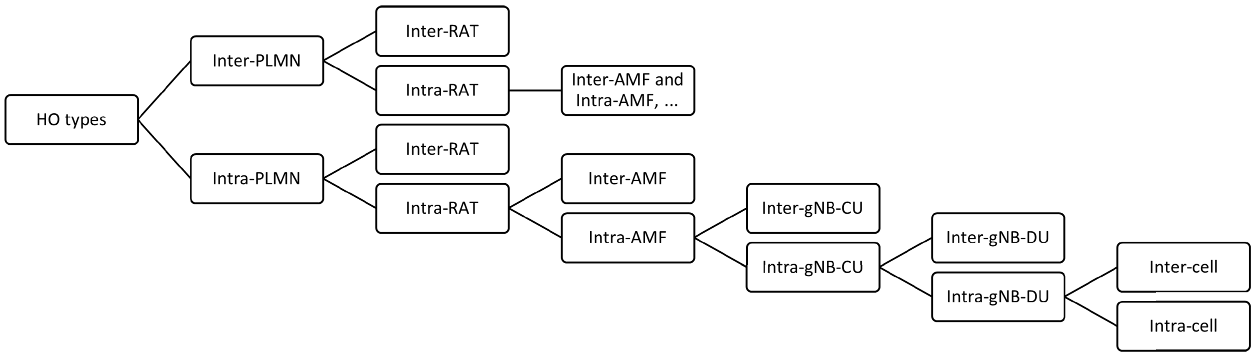

FIGURE 2. Handover types in 5G-NR [14], [16], [24].

A UE may send measurement reports in a time-based or event-based schedules. According to the latest technical specification of 3GPP for RRC protocol in Subclause 5.5.4 of [13], 19 different type of events are considered for 5G network. These mobility events including A1 to A6 (for intra-RAT measurements), B1 and B2 (for inter-RAT measurements), I1 (for interference measurement), C1 and C2 (for sidelink channels), X1, X2, Y1, and Y2 (for L2 U2N relay measurements), D1 (for location or distance measurements), CondEvent T1 (for time measurements), and two voids for future developments. Each of the above mentioned measurement events has different application and can be used by the network to either initiate a HO or cancel the previously initiated one.

D. CONDITIONAL HO AND DUAL ACTIVE PROTOCOL STACK

To increase connection stability and protect users from abrupt disconnection from the network, Conditional HO (CHO) is included in 3GPP standards. In CHO, the gNB-CU's RRC sends conditions of a HO to the UE and candidate cells. So, when the conditions are met, the UE will decide and HO to one of the candidate cells as specified in Subclause 9.2.3.4 of [15]. For instance, if the signal quality from the source cell suddenly drops and UE is unable to communicate with the source cell, the UE could still switch to a candidate cell and preserve its connection with the network. In part of any HO procedure, the UE's data transfer might be interrupted till the UE is successfully transferred to a target cell. This interruption time is known as the Handover Interruption Time (HIT) or Mobility Interruption Time (MIT) and it is targeted to be zero millisecond for 5G [20], [26].

The Dual Active Protocol Stack (DAPS) HO is introduced to 5G by 3GPP to achieve zero HIT [15]. In DAPS HO, the UE stays connected to the source gNodeB and continues the downlink and uplink data transfer until random access procedure to the target gNodeB is established successfully. Although the HIT is aimed for zero millisecond, the HO procedure still consumes the network resources and network developers are trying to get as close as possible to zero millisecond [27]. Therefore, immense number of HOs impose a considerable communication and processing burden to the network and air interfaces (Uu links between UEs and NG-RAN). Moreover, DAPS HO is still subject to failure because of the wireless channel characteristics and high mobility users.

In summary, each time a user moves to a new cell in 5G, a new channel must be assigned to the user via a HO procedure. In this procedure, multiple messages need to be transferred between a UE and various network nodes that consume network resources, which may negatively impact user data transfer, and connection reliability. The reduction of cell sizes, significant increase in number of users, and higher mobility of cars and trains, further increase the number of HOs and magnify its negative effects. Therefore, procedures are needed to reduce the number of HOs, improve the HO procedure, and use more reliable and seamless HOs for high-speed users in order to improve network performance and reliability.

III. RELATED WORKS

As a consequence of frequency reuse, handover is an inevitable procedure in cellular networks that helps to provide high QoE for users. Despite all the HO procedure modifications in each of the cellular network generations (2G to 5G), there are still more room for enhancement and adaptation to the new environment. Researchers try to optimize the HO procedure, minimize the HIT, reduce HO failure, diminish the number of HO requests, and make the HO process imperceptible for users.

In [28], the authors model the HO process as a contextual multi-armed bandit problem. They optimize the HO between 5G base stations in a centralized unit using the Q-learning method, based on user's RSRP. Their agent chooses proper HO action using the measurement reports from the UEs and achieve better link-beam gain. Random Access Channel-less (RACH-less) HO and make-before-break HO are two techniques to decrease HO latency. In [26], to achieve seamless mobility and reduce the HO latency, the authors propose HO without requiring a synchronized network or random access channel. To reduce the HO failure rate and decrease the HIT in 5G mm-Wave network, Baik and others in [29] proposed a

HO scheme based on deep learning that uses soft HO, multi connectivity, and downlink control to achieve this goal.

To reduce the number of HO requests, the authors in [22] group a few cells together and form a virtual cell for each user and use joint transmission from these cells. However, their joint transmission over different cells have the multipath interference issue. Since this method uses multiple transmissions from different cells, it is not applicable in the mm-wave frequency range due to the high propagation losses in these frequency ranges. Also, for high speed users, their algorithm either needs users' future mobility information or it imposes considerable processing overload to the network for virtual base station formations because of the user's short presence at each cell. Calhan and Cicioglu in [30] consider RSSI, Bit Error Rate (BER), and Outage Probability parameters and used fuzzy logic to reduce the number of HOs in 5G dense networks with NOMA medium access control. Since they considered 5G small cells, using the NOMA technology will cause huge waste of power resources as the difference between required power for near and far users are not considerable. Therefore, the network must waste lots of power for Successive Interference Cancellation (SIC) which make it impractical.

For interference management and HO reduction in 5G vehicular small-cell network, the authors in [31] use the NOMA scheme and mobility-aware cell association. Their objective are to maximize long-term network-wide data rate and increase user presence at serving cell to reduce HO. The issue of platoon HO authentication in Vehicular Ad-hoc NETwork (VANET) is investigated in [32]. The platoon head vehicle, on behalf of the fleet, communicates with a SDN controller to facilitate the authentication process and reduce platoon signalling overhead. In [33], a hierarchical clustering of 5G users based on their proximity is proposed to reduce the HO rate that is very similar to the IAB-node concept used in the 3GPP standard [16] or the Vehicular CrowdCell proposed by BMW in 2016.

The 3GPP standard for 5G, supports Non-Terrestrial Networks (NTN) in NG-RAN architecture. The NTN uses space-borne vehicles (Low and Medium Earth Orbit - LEO and MEO satellites) or airborne vehicles (unmanned aircraft systems) [34]. LEO satellites are orbiting earth at very high speed and their location in the sky change rapidly. Hence, non-terrestrial communication links are challenging due to far distance and constant movement of satellites that negatively affect the performance of HO procedure for 5G over NTN networks. In [35], a HO procedure is proposed for 5G over LEO communication based on the predictable movement trajectory of satellites to reduce unnecessary HOs and HO failures in NTN network.

Saritha et al. in [36] propose a channel reservation procedure based on learning automata and node speed. Their method needs the position, speed, and signal strength of the vehicles to estimate the HO time. Then, according to these data, their algorithm predicts and reserves a channel before the vehicle reaches the HO point. This algorithm needs to monitor the accurate position of each vehicle with precise timing. Hence, its processing cost is high and needs extensive collaboration of base stations to plan for all vehicles. In [37], Lee and others propose a deep reinforcement learning-based DAPS HO procedure to prevent the HO failure in mm-Wave 5G network.

Optimal channel allocation in VANET and 5G networks is critical due to limited availability of wireless resources, the stringent service quality requirements, and for reducing the number of HO to improve network performance. Zhou in [38] proposed distributed joint channel allocation and rate control to maximize the network throughput in VANET. In [39] hierarchical resource allocation based on the Nash bargaining game is proposed. At the first level, they distribute the spectrum from the central cloud between RSUs. Then, deal with spectrum sharing between vehicular users in RSUs. Channel assignment in vehicular network based on the road is studied in [40]. In this paper, the authors proposed Multi-Interface Multi-Channel (MIMC) road-based assignment method by modelling the road as a line. Then, the authors assign each part of a road to a specific channel (repetitive pattern) and decide about the HO time based on vehicles location and speed.

All the above mentioned papers help to improve the HO procedure, optimize the channel allocation or HO initiation time, or improve conditional HO process. However, to the best of our knowledge, there is no practical proposal for high-speed users of 5G small cell network with mm-wave frequency range with the objective of HO reduction.

IV. SYSTEM MODEL

In this paper, we consider the 3GPP-based 5G network with FR2-supported (mm-Wave band) small-cells (RSUs) installed alongside the road as shown in Figure 3. A two-way straight road with one or more lanes in each direction and sidewalks on both sides of the road is the base of our environment consideration. In this paper, RSU and cell terms are used interchangeably and both refer to a 5G small-cell with FR2 frequency range. RSUs are located in the road median and each RSU services both directions of the road. The road may have one or more lanes in each direction. One gNB-DU controls multiple RSUs (cells) and multiple gNB-DUs are connected and managed by one gNB-CU. A gNB-CU and its connected gNB-DUs form one gNodeB (one node of the NG-RAN) as is explained in Section II and shown in Figure 1. Each RSU covers a few tens of meters (ISD=50m and 100m according to Tables 6.1.8-1 and 6.1.9-1 of [20]) around itself with slight overlap with neighbour cells.

As we are considering the split-cell model of the gNodeBs, it is assumed that cell antennas are installed in lampposts without loss of generality. The gNB-DUs are distributed alongside the road to minimize communication delay on time sensitive protocols. As gNB-CUs are hosting time-insensitive functions, they could be located away from the road in a central powerful server hosted by a hypervisor. However, the installation location of the RSUs and other network nodes

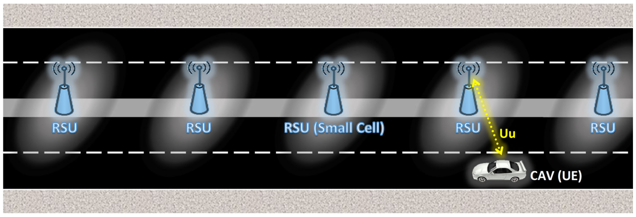

FIGURE 3. General view of the considered road and RSUs alongside the road in the road median.

have no negative impact on our proposed scheme. So, RSUs can be located on one side of a road, on a road median, in a dedicated cellular tower, or in a lamppost. It should be noted that our proposed model is in accordance with option 2 of [20] (macro-cell and RSUs) in highway and urban scenarios for connected cars with the focus on RSUs. However, the macro-cells provide additional coverage and support for users without any interruption to the proposed scheme.

The gNodeBs are connected to their neighbours through the logical Xn interface and cells in each gNodeB are logically connected together through their gNB-DUs and eventually their gNB-CU [41]. Hence, gNodeBs can communicate and collaborate with each other to reserve/release a channel, inter-cell interference coordination, and HO procedure communication. So, all RSUs alongside a road are logically connected together and could share information with their neighbours if it is required.

We assume RSUs are using mm-Wave bands because of higher bandwidth availability in these bands and also its high absorption ratio by materials that reduces the effect of multipath signals and interference. In our model, we assume all 5G UEs and devices inside a vehicle are connected to a central unit in the vehicle and all their data traffic passes through a shared link between the vehicle's central unit and the network. In this case, vehicles behave as relays for other 5G mobile devices and equipment as explained in clause 6.1.6 of [16]. It should be noted that addition of MIMO antenna and digital beamforming to the assumed RSUs and CAVs could help to narrow beams which reduce co-channel and adjacent channel interference considerably. Also, MIMO and beamforming can further improve the frequency reuse ratio and QoE for users.

V. MOBILITY MANAGEMENT FUNCTION

In this section, we briefly review the conventional mobility management (in 5G) as described in the 3GPP's documents and then present our proposed mobility management function.

Mobility Management Function (MMF) is one of the main functions of the RRC protocol in a gNB-CU for a UE in RRC_Connected state. The mobility management function in RRC is functioning based on the measurement reports from a RRC_Connected UE. The mobility management is a complicated function with many special cases, but here we present a simplified model to provide a general idea about how it works. In Figure 4-(a), an abridged flowchart of the conventional MMF is depicted.

The UE's measurement report could be either a timely scheduled or an event triggered message. For interval reports, once a UE sends a measurement report message to its serving gNodeB, the RRC checks the received signal quality. The RRC compares the measurements from the serving and neighbour cells with equivalent thresholds to take action and decide if HO is required. In cases that the message is a HO cancellation report (such as A1 that shows serving cell condition is improving), the MMF might decide to cancel an ongoing HO procedure for this user. On the other hand, if the report is one of the HO initiation events or a timely scheduled report with the low serving cell's signal strength measurement, the MMF needs to investigate the condition and make decision about the HO or parameter adjustment. The MMF might ask the serving cell about the recent configurations and maybe decide to wait for the next reports or adjust some parameters. If it finds that non of the other options help, it compares the serving and neighbours' received signal quality and decides to HO to a new channel. At this stage, if the HO is required, the MMF determines the HO type and selects a target cell accordingly, and then starts communicating with the target cell for the HO.

The proposed mobility management function is the expansion of the traditional MMF. The new MMF is achieved by the addition of our proposed VFR scheme and cell reselection procedure to the conventional channel allocation scheme and HO procedure. The simplified flowchart of the proposed MMF is shown in Figure 4-(b). The proposed MMF can be used in any gNodeB to manage low-speed users with negligible added processing overhead (just one speed comparison is added in the low-speed process). It also supports high-speed users with the VFR scheme using the conventional 5G infrastructure.

Similar to the conventional MMF, the starting point is the top of Figure 4-(b) using the measurement report from a UE; it is only applicable to UEs in the RRC_Connected state. Each time a gNB-CU receives a measurement report message, it runs the message through the MMF, completes a loop in this flowchart and waits for the next message from a UE. The first action after receiving a message is to check for the event triggered report or a weak signal strength. If the message is a timely scheduled measurement report and the reported signal quality (RSRP, RSRQ, SINR, or etc.) is strong enough, then the RRC takes no action and waits for the next report. As it was mentioned in Section II-C, some of the measurement events are used for HO initiation (such as A4 or A6) and some are used to cancel an on-going HO procedure (such as A1). In case of a HO cancellation event message, it proceeds to cancel an on-going HO procedure for this user as the condition in the serving cell is improving. If one of the HO/cell-reselection triggering events occurs or the serving cell's signal quality is below a given threshold, then the proposed MMF investigates the condition and makes

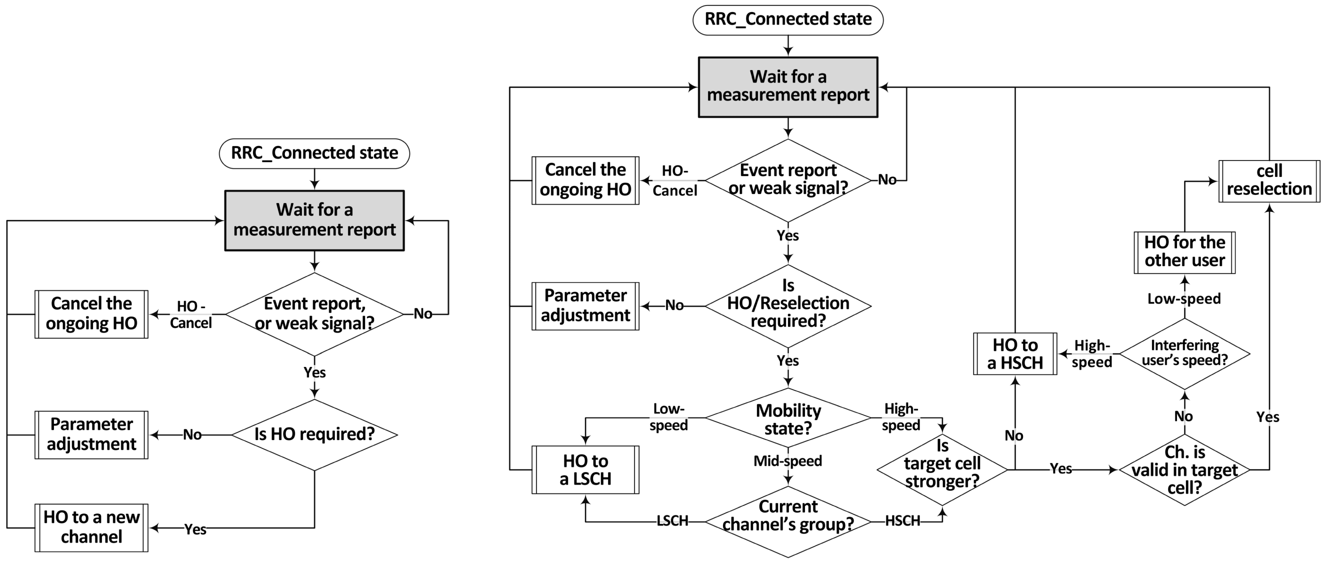

(a) The conventional MMF (b) The proposed MMF

FIGURE 4. **Flowcharts of the conventional and proposed mobility management functions.**

a decision. The MMF may adjust parameters (e.g., transmit power or antenna beams) or initiate a HO or cell reselection.

For this purpose, the gNB-CU might request the source gNB-DU for current configuration and then use all the available information to decide if parameter modifications such as increasing transmission power, decreasing interfering channels' power, new measurement setting for the UE, or other changes could solve the problem.

If HO/cell-reselection is required, the proposed MMF will check UE's mobility state. It should be noted that for a user in the 5G three mobility states are defined namely normal-mobility, medium-mobility, and high-mobility (subclause 5.2.4.3 of [23]). According to the 3GPP standard, a UE's mobility state is defined based on the number of cell reselections during a period of time. However, we define new mobility states based on users speed namely low-speed, high-speed, and mid-speed in each direction of the road. Our proposed mobility state determination strategy is more agile and adaptive to users' rapid mobility changes while the 3GPP's model is based on the users' long term behaviour. The low-speed users in both directions of the road are treated the same since they use the same set of channels. However, to avoid excessive HOs, the high-speed users in each direction of the road use a separate set of channels, but all users still use the same RSUs. Therefore, the separation benchmark for high- and low-speed users in positive and negative range of velocities could be different as further discussed in Section IX. The mid-speed mobility state is a temporary state defined for users in the hysteresis range around the speed separation benchmark ($VT \pm Hyst$). It helps to avoid unnecessary HOs for a user with speed around the separation metric since the user might dwell around the decision making point and require HO frequently. Defining a hysteresis parameter protects the network from these nonessential HOs.

A high-speed user that is managed by our channel allocation scheme (VFR scheme) is called a HSU and a low-speed user that is using a conventional cell-centric channel allocation scheme is known as a LSU. To avoid superfluous HOs, it is recommended that these two groups of users (HSUs and LSUs) use separate sets of channels. A set of channels used for HSUs by the proposed VFR scheme is labelled as HSCH-list and a single channel in this list is named as a HSCH (High-Speed users' Channel). Likewise, a set of channels used by LSUs is called LSCH-list and one channel in LSCH-list is a LSCH (Low-Speed users' Channel).

Since mm-Wave bands have short range propagation distances, HSCHs can be reused for a LSU in a short distance away from the road, e.g., in a femtocell inside a building or other residential areas. Therefore, the separation of channels (LSCH and HSCH) is only required around roads and highways and HSCH channels can be reused for slow users just a few hundred meters (or less) away from the road. The broad bandwidth in the mm-Wave frequency ranges alongside with Dual-Connectivity (DC) and Carrier-Aggregation (CA) technologies allow high data rate transmission for users. Therefore, a HSCH channel using these technologies can handle the required high data rate for a vehicle itself and all passengers' equipment in it. So, the traffic aggregation of passengers in their vehicles can further help to reduce the HO rate and control plane traffic load.

According to Figure 4-(b), if the MMF has already initiated a HO for a UE in low-speed mobility state, the MMF starts a HO procedure for this user with a channel from the LSCH-list. For a user at mid-speed state with weak signal quality (at the bottom of Figure 4-(b)), the best approach is keeping it in the same channel group as it is now (either LSCH-list or HSCH-list since there is no channel list for mid-speed users). In other words, if it is a LSU with a LSCH, it gets a new channel in the same group and if its current channel is a HSCH, it is treated as a HSU again. So, the MMF starts a HO procedure with a channel from LSCH-list for a mid-speed user that is currently using a LSCH. We recommend that if a user does not have a speed measuring instrument and cannot report the speed, it is considered as a LSU while all cars have access to their speed and can report it (we ignore the security aspects in user reports). A mobile user without a satellite positioning technology (such as a GPS) is very rare, but it could be applicable for other connected devices such as home appliances or other similar fixed 5G equipment or IoT (Internet of Things) devices.

The right side of the central stem of Figure 4-(b) is related to HSUs (the proposed VFR scheme). If the user is clustered as a HSU by the MMF and has a weak signal, the next step is checking the signal condition in the target/neighbour cell. If the neighbour cell's signal is also weak, then HO is inevitable and the user will get a new channel from the HSCH-list. However, if the reference signal in the target cell is stronger than a given threshold, the MMF checks to see if the user's channel is available in the target cell or there is another interfering user in a distance-threshold cell away from the target cell. If the channel is not available in the target cell (i.e., there is another HSU with the same channel - interfering user), the MMF communicates with that interfering user's gNB-CU (if these two HSUs are serviced by two gNB-CUs) and checks its latest reported velocity. The interfering user might have already reduced (or completely stopped in the middle of a cell) its speed below the threshold for HSUs. So, if the interfering user is no longer in the HSU's speed range, then that user should get a new channel from the LSCH-list in its own cell. Now this user can proceed to the target cell without HO and the cell-reselection will be executed after the HO of the interfering user. On the other hand, if the interfering cell is still in the HSU's speed range, the current user needs to HO to a new HSCH from the available channels in the target cell's list. Lastly, if the HSU's current channel is available in the target cell, then the VFR cell reselection procedure between source and target cells begins and the user will keep its own channel.

As the HSUs' paths are predictable because of the roads predefined trajectories, the network can have a list of possible target cells for the user based on its current and previous cells. This predictable path helps the network to better set the HO threshold and have enough time for decision making and reducing the chance of connection loss which is critical for high-speed users. The UE's measurements from these candidate cells help the network to decide about the target cell and starts the cell reselection procedure before the user enters the target cell. It is worth noting that communication with the user and getting its trajectory also could help the network to plan ahead of time and decide more confidently. However, this will increase the communication overload and it is out of the scope of this paper. Therefore, in this paper we focus on target cell selection based on the user measurement reports.

The proposed MMF might look complicated, but the implementation is very simple and the processing overhead is negligible. Algorithm 1 illustrates the proposed MMF's implementation that helps to further clarify our MMF model in Figure 4-(b) and also prove the simplicity of its implementation.

Algorithm 1 The Proposed Mobility Management Algorithm

```
if (HO_Cancellation_Event) then
    Cancel the ongoing HO
else if (Thld_m < P_RS) ∧ (P_RS < Thld_S) then
    Parameter adjustment
else if (P_RS < Thld_S) ∨ (HO_Event) then
    H_flag ← 0
    if (V_U < VT − Hyst) then                      ▷ Low-speed
        HO to a LSCH
    else if (V_U > VT + Hyst) then                 ▷ High-speed
        H_flag ← 1
    else                                           ▷ Mid-speed
        if (C_U ∈ HSCH_list) then                  ▷ Mid-speed, HSCH
            H_flag ← 1
        else                                       ▷ Mid-speed, LSCH
            HO to a LSCH
        end if
    end if
    if (H_flag = 1) then                           ▷ HSU
        if (P_RT < Thld_T) then                    ▷ Weak target cell
            HO to a HSCH
        else                                       ▷ Strong target cell
            if (C_U ∈ T_list) then                 ▷ Valid ch. in target cell
                VFR Cell Reselection
            else if (V_I < VT − Hyst) then         ▷ LSU int.
                Int. HO to a LSCH
                VFR Cell Reselection
            else                                   ▷ High-speed interfering user
                HO to a HSCH
            end if
        end if
    end if
end if
```

In Algorithm 1, P_{RS} stands for the received power from the source cell, $Thld_S$ is the threshold for source cell signal strength level, and $Thld_m$ is the minimum critical threshold for HO initiation. For the HO/cell-reselection event message for a UE, the *HO_Event* and *HO_Cancellation_Event*, respectively, represent the initiation and cancellation event reports. The H_{flag} is an algorithm internal flag for HSU detection and it is set if either UE's current speed is high enough or UE's mobility is in mid-speed state, but user's current channel is from the HSCH-list. The V_U is the UE's velocity and V_I is the interfering user's velocity, VT is the Velocity-Threshold, $Hyst$ is the velocity hysteresis value set by the network to reduce unnecessary HOs. The parameter C_U is the UE's current channel, and $HSCH_{list}$ is the list of all high-speed channels dedicated to the VFR scheme (HSCH-list). The P_{RT} is the received power from the target cell, $Thld_T$ is the threshold for target cell signal strength level, and T_{list} is the list of all available channels in target cell at the moment.

According to Algorithm 1, if the message is not an event triggered message or the reported signal strength is strong enough to keep the user connected the proposed MMF takes no action and waits for the next report message. For *HO_Cancellation_Event* message, the MMF proceeds to cancel the ongoing HO procedure for this user. In situations when the received signal is weak (less than $Thld_S$), but is still not in a critical low situation ($P_{RS} > Thld_m$), the MMF tries to improve the condition by parameter adjustment or obtain more information by measurement report's configuration changes. If the UE's received signal is weak and HO/cell-reselection is required, the MMF checks UE's mobility state by comparing the reported velocity with the hysteresis ($Hyst$) range around the Velocity-Threshold (VT) value. The MMF clusters the UE in one of the low-, mid-, or high-speed states according to its reported velocity. For a mid-speed user, the MMF clusters this user in one of the two states of low-speed or high-speed groups based on its current channel group (C_U), not the user's velocity. The current channel is either LSCH or HSCH and correspondingly the user is clustered in either low-speed or high-speed groups. The hysteresis ($Hyst$) can be zero if there is a big gap between velocities in low-speed and high-speed groups or the number of HOs due to users speed flickering around the velocity-threshold metric is negligible.

Once the algorithm detects a UE as a low-speed user with weak signal, the UE obtains a LSCH through a standard HO procedure. The HO type (inter-cell, inter-gNB-DU, inter-gNB-CU, etc.) is selected based on the source and target cells arrangements as explained earlier. For HSUs, when the MMF algorithm detects a HSU with a weak signal and sets the H_{flag} flag, a few more steps are still needed to decide whether a HO procedure or VFR cell reselection is required. If the target cell's received signal level is not strong enough ($P_{RT} < Thld_T$), then HO is unavoidable. Otherwise, the MMF checks the validity of the user's channel in the target cell. If it is available in the target cell ($C_U \in T_{list}$), the UE keeps its channel and a VFR cell reselection occurs between cells. However, if the user's channel is not available, it means that there is an interfering user for this channel in the target cell and the interfering user's speed determines the HO or cell-reselection for this user. If the interfering user's last reported speed is less than the speed threshold for HSUs ($(V_I < VT - Hyst)$), the interfering user must do a HO to a channel in LSCH-list and this user continues with only a cell-reselection. Otherwise, the interfering user keeps its channel and this user changes its channel to a new HSCH through a HO procedure.

VI. CELL-RESELECTION

In this section, we briefly review the most common HO signalling procedure in the RRC_Connected state and then present our proposed cell-reselection procedure for the suggested MMF with VFR scheme.

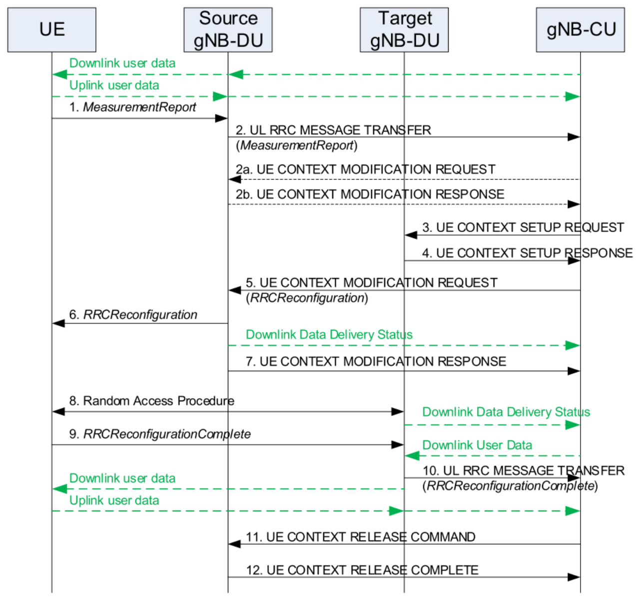

FIGURE 5. Inter-gNB-DU Mobility for intra-NR (Figure 8.2.1.1-1 of [16]).

Since each gNB-DU has multiple cells and each gNB-CU controls several gNB-DUs, two of the most common HOs are intra-gNB-DU and inter-gNB-DU. The inter-gNB-DU HO signalling for 5G-NR presented in Figure 8.2.1.1-1 of [16] is shown in Figure 5 and described below for ease of comparison with the equivalent proposed cell-reselection procedure. As explained earlier, the HO procedure starts with a measurement report message from a UE to its source gNB-DU (step 1) which is then passed by the gNB-DU to the serving gNB-CU (step 2). The gNB-CU may query the latest configuration from the source gNB-DU by sending the "UE CONTEXT MODIFICATION REQUEST" message and to obtain a response (steps 2a and 2b). At steps 3 and 4, the gNB-CU communicates with the target gNB-DU with HO preparation information and requests to create an UE context and set up a channel for this user. After target gNB-DU's confirmation, the gNB-CU sends the context modification message to the source gNB-DU which includes the new RRC configuration for the UE (step 5). The source gNB-DU passes the RRC configuration message to the UE and also informs the gNB-CU about the status of downlink data delivery (unsuccessful deliveries) to UE and context modification at steps 6 and 7. The UE with the new RRC configuration for the target cell, starts the connection process to the target cell and inform it after the completion of the configuration (steps 8 and 9). At this point, the UE is connected to the target cell with new channels and resumes its downlink or uplink data transmission while the target cell informs the gNB-CU about the successful HO procedure (step 10). The gNB-CU sends the resource release command to the source gNB-DU after receiving the successful HO confirmation message from the target gNB-DU (steps 11 and 12). In inter-gNB-DU mobility procedure, during steps 5 to 10, the UE data transmission is suspended till the new channels are established in the new cell.

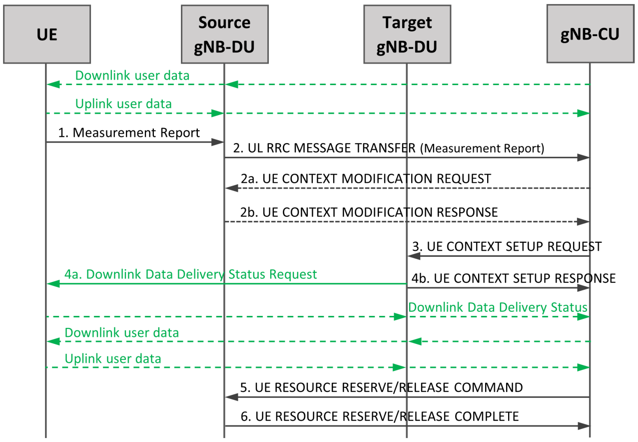

FIGURE 6. The proposed cell reselection for a VFR scheme user during an inter-gNB-DU mobility.

The intra-gNB-DU HO (including intra-cell HO) procedure has less signalling steps than the above explained inter-gNB-DU HO, but it is very similar to Figure 5. That is due to the fact that the intra-gNB-DU HO procedure occurs between a UE, a gNB-DU (both of the target and source gNB-DUs are the same), and a gNB-CU. During the intra-gNB-DU HO, although the entire UE mobility is happening within one gNB-DU, the HO procedure is still managed by a gNB-CU and the signalling between gNB-DU and gNB-CU is required.

In contrast to the cell reselection in 5G which is only valid for RRC_Idle or RRC_Inactive states, the proposed cell-reselection is defined for a UE in the RRC_Connected state. The proposed procedure is considered as a cell reselection rather than a HO because no RRC configuration is required on the UE's side. Therefore, the entire procedure is imperceptible for the user and only happens on the network side. The proposed cell reselection is for a HSU in the RRC_Connected state that is controlled by the proposed MMF while using our VFR scheme. The proposed cell-reselection for a user in an inter-gNB-DU mobility is presented in Figure 6.

According to Figure 6, the proposed cell reselection procedure begins with the UE's measurement report message to the serving gNB-DU (step 1) and then the gNB-DU passes the message to the gNB-CU for processing (step 2). The gNB-CU may request the source gNB-DU for the latest configuration (steps 2a and 2b) and based on the available information makes decision on cell reselection (whether it is required or not) and the cell reselection type. If cell reselection is required and it is an inter-gNB-DU mobility, the gNB-CU requests the target gNB-DU to setup the context at the targeted cell. The gNB-CU also updates the resource reservation on the following a few cells (Distance-Threshold cells) as further explained in Section VIII (step 3). The target gNB-DU may request downlink data delivery status from the UE and inform the UE about its cell ID (step 4a) and also sends the setup confirmation to the gNB-CU (step 4b). The gNB-CU sends/receives the rest of the user data through the target gNB-DU. Finally, the gNB-CU informs the source gNB-DU to update the resource reservation in its latest Distance-Threshold cells (explained in Section VIII) and to release this channel for cells before them (steps 4 and 5).

As it can be observed in Figure 6, during the proposed cell reselection procedure, no RRC configuration message is sent to the UE. In the UE's perspective, only the serving cell's antenna is changing from one location to another while the channels remain the same.

In intra-gNB-DU mobility, the cell reselection procedure is following the same concept and similar to the equivalent HO procedure, only one gNB-CU and one gNB-DU are involved in the cell-reselection procedure. The same concept can be further expanded to the other mobility cases such as inter-gNB-CU or inter-AMF.

VII. VFR SCHEME

The proposed Vehicular Frequency Reuse (VFR) scheme is a novel user-centric channel allocation scheme for high-speed users in 5G network. This scheme reduces the number of HOs (HO rate), control plane traffic particularly on wireless links, facilitate servicing high-speed terrestrial users in 5G's small-cells, and increases the frequency reuse rate. As a result, link reliability and 5G KPIs (Key Performance Indicators) improve and network can support high-mobility users with small-cells at high frequency bands such as mm-Wave ranges. The proposed MMF is developed to add the VFR scheme to the conventional cell-centric channel allocation in 5G. The VFR scheme Users' mobility is addressed by either the proposed cell-reselection procedure or the conventional HO procedures depending on the conditions.

In the VFR scheme, a channel is assigned to a user and stays with it as the user moves from one cell to another. When a user in the VFR scheme moves between cells without changing its channel, the cell-reselection procedure re-configures the NG-RAN nodes' settings. This procedure changes the primary serving cell (PCell) for that user as it enters a new cell. In contrast, in the conventional cell-centric channel allocation scheme, every time a user moves to a new cell, it needs to change its channel and configuration alongside with updates in the network's setting through a HO procedure. That is because each cell has its own specific set of channels.

In the VFR scheme, a group of N HSUs with N diverse HSCH channels can be modelled as a virtual elongated cell in each direction of a road. This virtual cell is sliding through the chain of small-cells while the network adapts itself with the users location in each cell. There are more similar virtual cells in the same direction of the road with the same group of channels. The length of this virtual cell could be as short as the diameter of two small-cells (if $DT = 1$) or much longer if N is a large number. It should be noted that the VFR scheme treats each user independently and does not group vehicles, form a platoon, or assign channels based on their location in a group.

Generally, in each direction of a road, vehicles relative position with respect to each other, change fairly slowly as confirmed by average low standard deviation of the recorded vehicles' velocities in [42]. So, it takes a while for two vehicles with an identical channel in two different cells to get closer than the minimum threshold and need a HO. This hypothesis is valid in both conditions of crowded and low traffic roads. On a busy road where channels need to be reused at short distances, vehicles' speed are nearly the same and it takes time for two vehicles with identical channels to reduce their relative distance. Also, in a low traffic road, the rate of reusing a channel will be low and the distance between two vehicles with equal channels is long enough. So, it again takes a long time to get closer than the minimum distance threshold, even if their relative speed is considerably high.

Users in the VFR scheme may use one channel during their passage through multiple cells without a HO, but still the standard HO procedure is required occasionally at much lower rates than the traditional scheme. When a HSU in the VFR scheme moves from one cell to another without using a HO, the NG-RAN (a MMF in gNB-CU) uses the proposed VFR cell-reselection between these two cells to adapt the network with user's mobility and keep it connected to the network. A HO in the VFR is needed either when two users with the same channel get closer than a preset threshold to each other (investigated in Section VIII) or a user has a weak signal strength in a cell while the neighbour cells' signals are also weak. It is noteworthy that a very weak signal strength in the assumed small-cells with mm-Wave band and LOS link is less likely to occur, but should be considered.

For simplicity and better understanding of the VFR scheme, consider a one-way road with 5G coverage by small-cells equipped with FR2 bands (mm-Wave frequency range). All nodes (gNodeBs) in this NG-RAN are using the proposed MMF on their RRC to service both the LSUs and HSUs using the VFR and traditional channel allocation schemes. Assume that connected vehicles (CAVs) on the road are driving fast enough to be clustered in HSU group by the MMF and have a channel from the HSCH-list. Suppose a vehicle that was parked on the side of the road and was connected to the network by a LSCH, starts to move. This vehicle will keep using its current LSCH channel in its current cell and get a new LSCH channel if it enters a new cell while its speed is not high enough to be clustered as a HSU. Once the user's speed exceeds the velocity threshold and moves into a new cell, the proposed MMF will cluster this vehicle as a HSU and initiate the HO procedure for it with an available channel from the target cell's HSCH-list. Every time each of these HSUs moves from one cell to another, the network starts a cell-reselection procedure instead of a HO. If two vehicles with the same channel get closer than a given threshold (DT in Section VIII), a HO procedure is required.

The VFR scheme can be used for all 5G users, but it is more beneficial and effective in a network if it is used for high-speed users such as CAVs, trains, motorcycles, fast-riding bikes, or human-driven connected-vehicles. That is one of the reasons for separating HSUs from LSUs based on their reported velocities. This separation is only at the software level and all the LSUs and HSUs are connected and are using the same 5G infrastructure. The number of channels in each of the HSCH- and LSCH-lists are adaptively controlled by the network and may change over time to provide maximum QoS and QoE for all 5G users.

TABLE 1. Assumptions of the road parameters for highways and city roads.

Parameter	Highway	City
Cell coverage diameter	100 m	50 m
Road type	Two-way	Two-way
Intersection types	Merge, Misaligned	Any type
Lanes per direction	3	2
Avg. vehicle length	4.6 m	4.6 m
Min. distance between vehicles	20 m	5 m
Distance-Threshold	1 cell	1 cell

To investigate the frequency reuse model in the VFR scheme, consider Z unique channels assigned to the VFR scheme (HSCH-list). Using the VFR scheme, all vehicles throughout the entire length of the road could be covered by these channels as long as Z is not too small. The minimum number for Z depends on the cell sizes, number of road lanes, distance between two consecutive vehicles, the Distance-Threshold (DT in Section VIII), and some other parameters. To get a sense of it, two different road scenarios (highway and a city road) are considered in TABLE 1. In this table, the assumed minimum distances between vehicles are less than the road safety requirements. Using larger values for minimum distances will reduce the minimum number of required channels (Z), but we consider the future CAVs with advanced technologies. Based on the assumed values provided in TABLE 1, the HSCH-list of a 5G network with the VFR scheme needs only 72 channels ($Z = 72$) for highways and 120 channels ($Z = 120$) for the assumed city. This will service all high-speed users over the entire network's coverage area. Be mindful that pedestrians are using the LSCH-list which is a separate group of channels.

VIII. DISTANCE-THRESHOLD

In this section we derive and investigate a metric for the minimum permitted distance, called a Distance-Threshold (DT), between two CAVs with identical channels (from the HSCH-list) and tolerable level of co-channel interference. Then we evaluate the DT based on some realistic network parameters and simulate it for a range of SINR values in Section VIII-A.

The minimum distance between two users with the same channel is calculated based on LOS links and maximum tolerable interference level. The DT metric specifies the frequency reuse ratio which defines the minimum number of cells as a gap between two cells using a channel for two different users.

For instance, if DT is equal to n and the j^{th} cell (cell with the Cell ID of $CID = j$) is using the channel c_i, the closest cells permitted to reuse this channel are $CID = j \pm (n+1)$. While cells with IDs of $CID = \{j \pm 1, j \pm 2, \ldots, j \pm n\}$ must reserve channel c_i and cannot use it. Therefore, when a channel is used in the cell with $CID = j$, this cell will inform n cells on each side of it (through intra-DU, Xn link in inter-gNB, or N2 link in inter-AMF) to reserve this channel and not use it till future release message. The DT threshold is dependent on the number of antennas and their gains, beamforming, cell size, frequency range, RSU's antenna height, and tolerable SINR.

In this paper, we assume both the RSU and CAV are using efficient high gain antennas. The MIMO and massive MIMO antenna technologies considered for 5G and the addition of the adaptive beamforming can help to shape pencil beams and reduce the interference. Using these technologies can decrease the DT even down to zero, reduce the transmission power for the same signal quality, or improve the SINR. However, in this paper we consider fixed directional antenna patterns with small sidelobes, but without any adaptive beamforming. RSU's antenna patch is installed in lampposts of height h_{LP} and evenly spaced with a distance of d_{LP} from each other. To derive the DT, we shall start with the Friis formula. The Friis formula for free-space path loss with a large scale fading model, for our scenario between RSU and CAV, is given by (1).

$$P_r = P_t G_t G_r h_{ij} = P_t G_t G_r \left(\frac{\lambda}{4\pi d_{rt}}\right)^2 \quad (1)$$

In (1), P_r is the received power, P_t is the transmit power, G_t is the directivity of the transmit antenna, G_r is the directivity of the receive antenna, d_{rt} is the distance between the receive and transmit antennas, and λ is the transmit signal wavelength.

Using (1), the SINR (γ_{ij}) of the j^{th} RSU from i^{th} CAV in its coverage area with two co-channel interfering CAVs (one in the front and one at the back) is as follows:

$$\gamma_{ij} = \frac{P_{r_{ij}}}{\sum_{k\in N} P_{r_{kj}} + n_0} = \frac{P_{t_i} G_{t_i} G_{r_j} h_{ij}}{\sum_{k=1}^{N} P_{t_k} G_{t_{kj}} G_{r_{jk}} h_{kj} + n_0} \quad (2)$$

In (2), P_{t_i} is the i^{th} CAV's transmit power, G_{t_i} is the antenna gain of the i^{th} CAV in the main lobe, G_{r_j} is the antenna gain of the j^{th} RSU in the main lobe, h_{ij} is the channel gain between the i^{th} CAV and j^{th} RSU. Parameter P_{t_k} is the transmit power of the k^{th} CAV that causes interference for the i^{th} vehicle's signal in the RSU. Parameter $G_{t_{kj}}$ is the k^{th} CAV's transmit antenna's side lobe directivity in the direction of the j^{th} RSU. Parameter $G_{r_{jk}}$ is the j^{th} RSU's antenna's reception side lobe gain in direction of the k^{th} CAV. Parameter h_{kj} is the channel gain between the k^{th} CAV and the j^{th} RSU while n_0 is the noise power and can be calculated with (3).

$$n_0 = FkT_0W \quad (3)$$

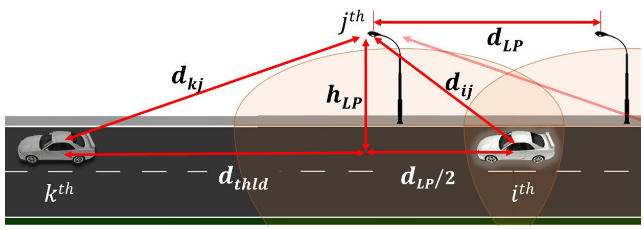

FIGURE 7. Section of the considered road with the i^{th} targeted vehicle and one the interfering vehicles on the left.

In (3), F is the receiver noise figure, k is Boltzmann's constant and equal to 1.38×10^{-23}, T_0 is the reference receiver temperature in degrees Kelvin (290°), and W is the receiver bandwidth. As we consider a section of a road without intersection and separated channel groups for each direction, in (2), N is equal to two. However, with an increase in N, this equation can be applied to different scenarios.

Substituting channel gain from (1) into (2) and considering $R_i = P_{t_i} G_{t_i} G_{r_j}$ and $R_k = P_{t_k} G_{t_{kj}} G_{r_{jk}}$ for simplicity, we obtain from (2)

$$\gamma_{ij} = \frac{R_i \left(\frac{\lambda}{4\pi d_{ij}}\right)^2}{\sum_{k=1}^{N} R_k \left(\frac{\lambda}{4\pi d_{kj}}\right)^2 + n_0} \quad (4)$$

According to Figure 7, the i^{th} CAV which is in the j^{th} RSU is using channel m and is served by this RSU. On the other side, the k^{th} CAV using the same channel m is ahead of the i^{th} CAV in a few RSU away from the j^{th} RSU and interferes with the i^{th} uplink signal. The distance d_{thld}, is the horizontal distance between the k^{th} CAV and the j^{th} RSU. In most extreme conditions, both interfering CAVs (in the front and at the back) are at the same distance of d_{thld} away from the j^{th} RSU, thus $d_{kj} = d_{1j} = d_{2j}$. By rearranging (4) with respect to d_{kj} and defining $C = 16\pi^2/\lambda^2$, we obtain,

$$d_{kj} = \frac{d_{ij}^2 \gamma_{ij} \sum_{k=1}^{N} R_k}{R_i - C d_{ij}^2 \gamma_{ij} n_0} \quad (5)$$

In the worst case scenario, the target vehicle (i^{th} CAV) is located at the j^{th} RSU's coverage edge and the two interfering vehicles are both at the DT span of the j^{th} RSU. Hence,

$$d_{ij} = \sqrt{h_{LP}^2 + d_{LP}^2/4} \quad (6)$$

$$d_{thld} \gg h_{LP} \qquad \therefore \; d_{kj} \approxeq d_{thld} \quad (7)$$

The distance between the i^{th} CAV and the j^{th} RSU when the CAV is at the cell edge is calculated in (6). According to (7), when the d_{thld} is considerably larger than the lamppost height h_{LP}, we could consider that d_{kj} is almost equal to the d_{thld}. Therefore, by replacing d_{ij}, d_{kj}, R_i, R_k, and C in (5) we get the DT equation.

$$d_{thld} = \sqrt{\frac{\left(h_{LP}^2 + d_{LP}^2/4\right) \gamma_{ij} \sum_{k=1}^{N} P_{t_k} G_{t_{kj}} G_{r_{jk}}}{P_{t_i} G_{t_i} G_{r_j} - \left(\frac{16\pi^2}{\lambda^2}\right) \left(h_{LP}^2 + d_{LP}^2/4\right) \gamma_{ij} n_0}} \quad (8)$$

The minimum distance between two consecutive CAVs using the same channel is presented in (8). This equation calculates the DT in meters which makes the network's implementation difficult as it needs an accurate location of each vehicle. So, we normalize it with respect to RSUs' (average) coverage diameter alongside the road and use the ceiling function to gain the least integer greater than or equal to the normalized DT. However, to do so we must add the RSU's coverage radius to the result of (8) because for the target j^{th} RSU, there is only a half cell on either side and we need to compensate for it. The average diameter of the cells (RSUs) is equal to the distance between two lampposts (d_{LP}).

$$D_{thld} = \left\lceil \frac{d_{thld} + \frac{d_{LP}}{2}}{d_{LP}} \right\rceil \tag{9}$$

The normalized distance threshold D_{thld} (DT=D_{thld}) expresses the minimum distance between two cells using an identical channel in terms of the number of cells. In other words, when a vehicle uses a channel in a RSU (j^{th} RSU), the closest vehicle with the same channel can be only DT RSUs away (in RSUs $j \pm (D_{thld} + 1)$).

A. DISTANCE-THRESHOLD EVALUATION

In this section, we evaluate the DT equation defined in (9) by considering realistic values for the parameters based on the literature and standards. Using computer simulation, we investigate the effect of antenna gains and transmission power on the DT and show the DT behaviour with respect to these key variables.

In deriving the DT equation, we assume that the radio units of gNB-DUs are installed in lampposts and they are equidistant from each other. According to Alberta's highway lighting guide [43], standard Davit pole heights in highways can be either 13.0 or 15.0 meters. The spacing between the lampposts is influenced by their location, luminaire, and other parameters that need to be designed and calculated accurately, but mostly ranging between 50 to 100 meters. In this article, we consider a 100-meter lampposts spacing ($d_{LP} = 100$) which is a logical spacing for small-cells serving high-speed users according to [20].

In addition to the RSU's location parameters, we need antenna directivity at each end of the wireless link and transmission power in CAVs. In [44], Tan and others analyzed three massive MIMO antenna arrays and investigated their directivity, maximum gain, sidelobe level, and beam pattern in mm-Wave bands. According to their research, these three types of antennas are almost identical. Hence, in this part we consider the UHPA (Uniform Hexagonal Planar Array) antenna for both RSUs and CAVs as a reference for our antenna parameters and get a sense of the DT values by simulation. The UHPA antenna has a maximum gain of 42.63 dB, beamwidth equal to 10.15 degrees and a sidelobe level of -18.86 dB. The other values of the parameters are based on the literature and are provided in Table 2.

The simulation of the DT's for a range of SINR from zero to 40 dB with other parameters as in Table 2, are illustrated in Figure 8. This figure shows that if we want to satisfy a SINR of 37 dB (or more) in the j^{th} RSU, there could be other vehicles using the same channel, as close as only two RSUs away (on $(j-2)^{th}$ and $(j+2)^{th}$ RSUs). However, in the real world and in the best case scenario, the received SINR in RSU is mostly less than 37 dB and the DT will be only one RSU between two users using a same channel. The DT equals to '1' means that if a CAV on the j^{th} RSU using the c_i channel, only one RSU on either side of the j^{th} RSU cannot use this channel for another user while the $(j-2)^{th}$ and $(j+2)^{th}$ RSUs may use the c_i channel for another CAVs.

TABLE 2. Parameter value assumptions for the distance-threshold simulations.

Parameter	Value	Unit
Lamppost height	15	m
Lamppost spacing	100	m
Transmit power (CAV)	8	watt
Maximum antenna gain	42.63	dB
First sidelobe level	-18.86	dB
Backlobe level	-25	dB
Frequency band	28	GHz
Noise Figure	8	dB
Bandwidth	100	MHz

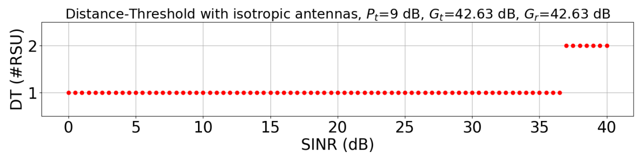

FIGURE 8. Distance threshold respect to SINR.

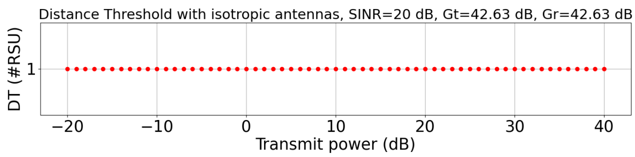

FIGURE 9. Distance threshold respect to CAV's transmit power.

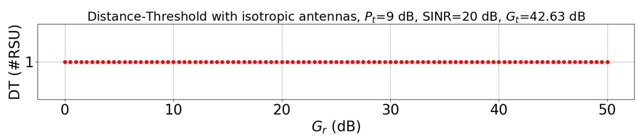

FIGURE 10. Distance threshold respect to the receiver antenna gain.

The plot in Figure 9 shows that the DT is independent of CAV's transmit power for a range of logical values for transmitting power.

The effect of reception antenna gain is the same as the transmit power, and a wide range of antenna gains does not affect the DT. The simulation of DT for a range of receiving antenna gains with SINR of 20 dB, transmit power of 9 dB and other parameters as Table 2, illustrated in Figure 10

IX. VELOCITY-THRESHOLD

This section presents the Velocity-Threshold (VT) metric that is used by the proposed MMF to separate low-speed and high-speed users. We also evaluate our metric in two datasets of mixed road users with large number of users based on a real recorded vehicle-speed dataset in combination with simulated pedestrian and cyclist speeds using real statistics from the literature.

Low speed group of users include all low-mobility mobile users such as pedestrians, slow-moving cyclists, electric scooters, and any other 5G users with a speed less than a threshold (VT). On the other hand, the HSU group covers all high-mobility wireless users such as CAVs, motorcycles, trains, human driven vehicles, and any other 5G terrestrial users with moving speeds higher than a threshold. To cluster cellular users based on their speed, the proposed MMF simply compares users' velocities with the VT (there could be also a hysteresis value included as we explained before) and cluster them into one of the two groups of the LSUs or HSUs.

Average road users' velocity in each section of a road may vary over time and have diverse values at different times of the day. It also changes from one day to another as it is dependent on many variables such as number of road users, weather conditions, or time of day. Applying a fixed user separation threshold for all times is not very practical or efficient. Also, finding an accurate mathematical model for this dynamic environment with variety types and shapes of roads, is very challenging and almost impossible. Therefore, we use a Machine-Learning (ML) algorithm to calculate the VTs according to the current conditions of a road. However, to keep the model simple and still effective, we only rely on users' reported velocities on our ML model, since the effect of all other variables (such as weather and road conditions) have already been reflected on users' speeds. Use of supervised learning algorithms needs a labelled training dataset for all different weather and road conditions which is not feasible. Hence, we use an unsupervised ML namely the K-Means clustering algorithm to find the VTs on separate sections of a road.

As it was mentioned before, each gNodeB (or gNB-CU) has multiple gNB-DUs and each gNB-DU controls several cells (RSUs) and there could be tens of user (cars and pedestrians) in each cell. So, each gNB-CU might be servicing hundreds of users, which means it has access to their velocities. Therefore, each gNB-CU has enough speed samples to find the VTs for its entire coverage area or divide its coverage area into multiple sections and find VTs for each part discretely if it covers variety types of roads. However, in continuous sections of a road for a gNodeB or in a road covered partially by multiple gNodeB, each gNodeB may communicate with its neighbours to align and adjust their VTs with each other. Then, the MMF in each gNB-CU, uses these VTs to cluster their users and assigns HSCH or LSCH channels accordingly.

Although the average speed of road users, particularly vehicles, changes over time, this change is normally very slow and needs at least a few seconds or more. Therefore, gNodeBs do not need to run the ML algorithm for each UE's report and calculate the VTs. For instance, if a gNodeB servicing 1000 high-speed users, a few speed changes barely affect the previously calculated VTs. This means that gNodeBs need to update their VT metrics over relatively long time intervals between each update. So, gNodeBs have enough time and processing resources for a simple K-Means algorithm. The K-Means algorithm needs to be executed only every few seconds while the MMF called probably thousands times in a second. It should be noted that the VT calculation process is independent of the mobility management process (MMF), but the resulting values are used by the MMF.

In our system, RSUs are located in the road median and support both directions of the road including pedestrians on sidewalks. That means, the reported speeds include both positive and negative velocities (for each direction of the road). So, after clustering them, at least three groups are required. This means two VT values are needed, one VT in the positive range to distinguish positive-speed vehicles from pedestrians and likewise one VT for negative speeds. These three clusters include one for LSUs (e.g., pedestrians with either positive or negative speed, parked vehicles, or stationary devices) and one cluster for each direction of the road for HSUs (positive and negative velocities).

The cost function for the K-Means algorithm is an average of the distance between reported velocities and their currently assigned cluster as given below.

$$J(c^{(1)}, \ldots, c^{(m)}, \mu_1, \ldots, \mu_K) = \frac{1}{m}\sum_{i=1}^{m} d\left(x^{(i)}, \mu_c^{(i)}\right) \quad (10)$$

In (10), $c^{(i)}$ is the index of the cluster to which the i^{th} sample point ($x^{(i)}$) is currently assigned. The parameter μ_k is the k^{th} cluster centroid and the $\mu_c^{(i)}$ is the centroid of a cluster that the i^{th} sample point is assigned. The parameter $d\left(x^{(i)}, \mu_c^{(i)}\right)$ is the distance between the $x^{(i)}$ sample point (the i^{th} user's velocity) and its assigned cluster centroid $\mu_c^{(i)}$ according to the $d(.,.)$ distance metric. The goal is to find centroid locations iteratively such that the optimization problem in (11) is satisfied.

$$\min_{c^{(1)},\ldots,c^{(m)},\mu_1,\ldots,\mu_K} J(c^{(1)}, \ldots, c^{(m)}, \mu_1, \ldots, \mu_K) \quad (11)$$

The most common and frequently used distance metric for K-Means algorithm is the Euclidean distance. In one dimensional dataset, the Euclidean metric in a K-Means algorithm sets the clusters' separation point (threshold) exactly at the middle point between two cluster centroids. The equal distance of a threshold from the centroids in a Euclidean-based K-Means is a useful clustering tool for databases with almost equal variances in each group of data points (cluster). However, it is not useful in our case where the HSU might have much higher variances (a wider spread of points around their mean value) of velocities than the LSU. There are many distance metrics that can be used for the K-Means algorithm, but each of them has its own use cases. For our application, the best distance metric is proposed in [45] which assigns more share of space to the centroids with larger values (higher variances at higher velocity ranges). This distance metric is provided in (12) for one-dimensional data.

$$d(x, y) = \frac{|x - y|}{\sqrt{|x| + |y|}} \tag{12}$$

As we are using only the users' velocities along the road (not the separated values on each axis of X, Y, and Z), there is only one scalar value per user that could be even quantized to reduce the Uu links' communication load. For additional simplification and reduction of wireless traffic load, the network can broadcast the VTs to all users and let them compare their velocities and just report their group (LSU, positive-HSU, negative-HSU) with only two bits. In this paper, we just assume that the speed comparison with VTs and clustering are performed in the gNB-CUs.

A. VELOCITY-THRESHOLD EVALUATION

In this section, the simulation results of the Velocity-Threshold calculation and users' clustering using the K-Means algorithm in a two-way road with sidewalks and pedestrians in both directions are presented. We use the HighD dataset presented in [42] as a real world's vehicle's velocity sample points that is recorded on sections of two-direction highways in Germany. As we do not have access to any database for pedestrians on sidewalks (low-velocity mobile users), we generate random velocity samples for pedestrians and combine them with the vehicles dataset. To have a realistic gait samples of pedestrians on sidewalks, we use the real pedestrian statistics on sidewalks provided in the literature to generate our low-speed velocity data points. To simulate pedestrian velocities, we use the normal distribution with an mean of 1.25 m/s and standard deviation of 0.3 m/s in all directions with positive and negative velocities based on the studies presented in [46]. The number of pedestrians per section of a road, is generated by a uniform distribution with an average of 20 and a standard deviation of 5 that includes positive and negative velocities.

The HighD dataset is a bird's eye view of almost 400 meters of highways in Germany with two or three lanes in each direction which includes 60 recordings in six different locations. It contains the location of each vehicle, their relative position and their velocity with a frequency of 25 Hz in sections of highways without tunnels and harsh weather conditions. We use track 25 of the HighD dataset for our simulations which is 412 meters of a highway with three lanes in each direction. As we are using the HighD dataset, their dataset's road condition (number of lanes, length of the observed section of the highway, and weather condition) is dictating our simulation road features as well. The observed 412 meter of a road can be covered with four small-cells where each has an average coverage diameter of 100-meter that is compatible with our system model assumptions in Section IV. In reality, a gNB-CU may consider more cells together to calculate the VTs in this kind of road, but we are limited to the available recording size.

The input data to the simulation process are unlabelled, which means that the clustering algorithm has no information about a data point (whether it is a pedestrian or a car). Therefore, the algorithm's input dataset is just a list of rational numbers (signed decimal values) representing users' velocities. The VT algorithm, clusters these data points into K clusters, where in this section $K = 3$ in Figure 11 and $K = 5$ in 12. To visualize the clustering results of our algorithm, we use distinct colour and symbol for each cluster's velocity points. All the simulations in this paper are implemented using the Python programming language.

Figure 11 shows the Velocity Thresholds (VTs) and clustering results of five random snapshots (frames) of the highway with randomly generated pedestrian velocities. The horizontal axis is the velocity of mobile users in meters per second and the vertical axis shows various time slots. In Figure 11, data points are clustered in three groups (LSU, HSU-positive, HSU-negative) with unique colour and symbol for each cluster. This figure also includes the VTs (two thick vertical lines in red) and the clusters' centroids (three thin cross symbols in cyan). User's velocity points in the cluster for HSUs with negative velocities (one direction of the road) are shown with $\curlyvee$ symbol and magenta colour, that includes the points on the left side of each frame in Figure 11. Users clustered in the positive-velocity-HSU group are shown with $\prec$ symbols in blue colour on the right side of each time frame. Finally, in the middle section of each time frame, the data points clustered by the algorithm as the LSU group are indicated with $\curlywedge$ symbol and green colour in Figure 11. As mentioned above, the VT values (separation threshold between clusters) are exhibited with two red vertical lines in each time frame of Figure 11. By comparing the left red line (VT for negative speeds) in different snaps of time along the vertical axis, we can see the importance of the adaptive adjustment of the VT over time. Moreover, by comparing the positive and negative VT at each instance in time, such as t_5 at the top of Figure 11, it can be observed that the VT can be very different for each direction of the road. It is because the average speed in each direction is independent of the other side.

On a road with multiple lanes in each direction, there could be two noticeably different flows of traffic in each direction where cars in one or two lanes are driving considerably faster than the other lanes on the same direction. Another instance of notable velocity difference between two groups of HSUs in one direction of a road could be the presence of a bike lane alongside of a road. In these scenarios, the algorithm could cluster users into five groups and calculate four VTs to even separate these two group of HSUs in each direction and decrease the number of HOs. These five mobility states could be named as HSU-high-negative ($\curlyvee$ in magenta), HSU-low-negative ($\curlywedge$ in green), LSU ($\prec$ in dark blue), HSU-low-positive ($\succ$ in light blue), and HSU-high-positive ($+$ in magenta) from left to right on Figure 12

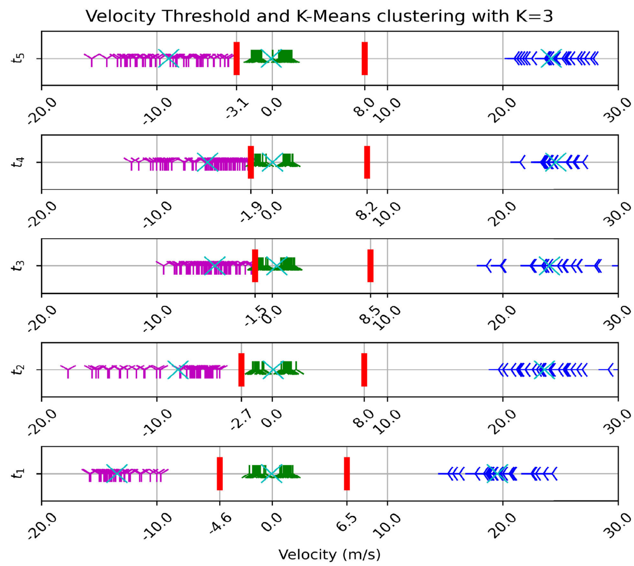

FIGURE 11. **Velocity threshold and K-means algorithm with three clusters in a two-way road for five random moment of time.**

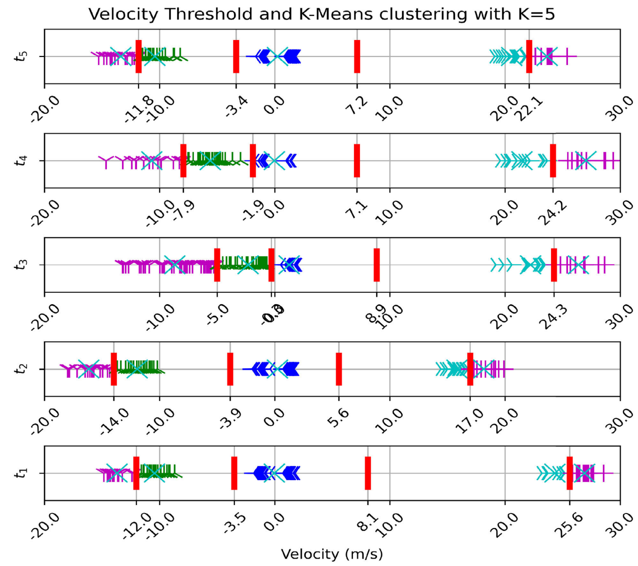

FIGURE 12. **Velocity threshold and K-means algorithm with five clusters in a two-way road for five random time slots.**

and along the horizontal axis. In this figure, five random occasions with various user-velocity ranges are presented and users are clustered into five groups. By comparing the clustering result in this figure, it could be concluded that in some cases using five clusters could be helpful but not always. In some conditions such as t_3 in Figure 12, we can observe pedestrians with negative velocities are classified in the HSU group that could increase the number of HO. In this case, using four clusters or merging green and blue clusters can solve the problem, but it increases the implementation complexity. In general, to select the optimal number of clusters K in the K-means algorithm, another algorithm with a cost function and optimization objectives to minimize the number of HOs can be used. However, that will increase the processing load and complexity. Therefore, there is a trade-off between the optimal number of clusters and implementation complexity. In most cases, $K = 3$ is a safe choice for the number of clusters on two-way roads and $K = 2$ is sufficient for one-way roads as we used on our MMF model.

As we mentioned earlier, in the VFR scheme, the VT values do not need to be update for each vehicle. In fact, it only needs to be updated once every few seconds, since the change rate of the average velocity in one direction of a road is low. Therefore, an occasional update of the VT metrics works just fine and protects the network from extra processing load and unnecessary HOs. The convergence time in the VT algorithm is very fast and in our simulations of the VT algorithm with the Python programming language. It converges in less than 17 milliseconds with a personal computer. However, in the 5G network it is expected that the algorithm is implemented in machine languages such as C and optimized to run much faster than our simulation Python code. Moreover, in powerful and high performance gNB-CU machines, the convergence time could be considerably less than our simulation time. As a result, the computational time of the VT processing time is considerably less than the required update rate and the network can easily handle the processing load of the proposed algorithm.

X. PERFORMANCE COMPARISON

To demonstrate the performance improvement of the proposed VFR scheme in comparison with the conventional channel allocation scheme, we compare the number of HOs in a section of a two-way road with two lanes on each direction. This road is serviced with small-cells (RSUs) and each RSU has 100 meters coverage radius as is shown in Figure 3. RSUs are using 26 GHz frequency band (FR2-1) with Time Division Duplex (TDD) mode and 100 MHz channel bandwidth. The 26 GHz frequency band's range is 24.250 - 27.5 GHz, that is 3.250 GHz bandwidth for both uplink and downlink that could provide 32 channels with 100 MHz bandwidth. So, in both schemes 32 channels are used to service all users. That means the HSCH-list of the VFR scheme has 32 channels in it. In these simulations, we do not consider any LSU as the VFR scheme is defined for only HSUs, but if there were any LSUs, they would have been using different frequency bands. Also, the Distance-Threshold for the VFR scheme is equal to one ($DT = 1$) in all simulation of this section while the VT is irrelevant as we only consider the HSUs in this part.

As it is mentioned in Section III, there is no other method to reduce the number of HO in 5G small-cells with mm-Wave bands for high-speed users. Therefore, we compare our proposed method's performance with the existing 5G mobility management scheme, according to the 3GPP's model, which is called as conventional networks in this paper.

According to the conventional networks, each time a user moves from one cell to another, it gets a new channel through the HO procedure, which is exactly how we find the number of HOs for traditional networks in our simulations. We neglect the intra-cell HOs caused by physical barriers, multipath and small-scale fading, because in our assumed model with small-cells and mm-Wave bands, the chance of intra-cell HO is low and has equal effect on both compared methods. So, it can be removed from both results without affecting their relative comparison result.

The location of vehicles on this road is generated randomly with realistic features. Each vehicle has at least 2 seconds of safety distance from the other vehicle ahead of it in the same lane in accordance with the road safety rules. The entrance time of vehicles in each lane follows a gamma distribution with shape and scale parameters equal to one in addition to the two seconds safety space to be more realistic and compatible with random behaviour of vehicles. We used gamma distribution for vehicle spacing because autonomous cars should keep the minimum two seconds distance from the car ahead and this distance cannot be negative. So there should be no tail on one side of the distribution. On the other side, to optimize fuel economy and road efficiency, CAVs need to minimize their spacing which would be close to two seconds distance. Therefore, the gamma distribution is a good choice to keep cars as close to each other as possible and still have random behaviour. The average velocity of all CAVs is 110 km/h (30.56 m/s) while the start and end velocity of each vehicle is generated using a normal distribution of mean 30.56 m/s and standard deviation of one. Therefore, each vehicle can change speed while passing this section of the road. The total simulation time depends on the number of RSUs, number of vehicles, and their velocities.

Figure 13 compares the number of HOs for different number of road users (CAVs) in a section of the road serviced by 10 RSUs in the road median. As the difference between the number of HOs in the traditional network and our proposed metric is considerably large, we used a logarithmic scale on the y-axis. For traditional networks, the number of HOs is equal to the number of vehicles multiplied by the number of RSUs. So, it linearly increases with the increasing number of users or number of RSUs. On the other hand, in our proposed scheme, HO is only required if two HSUs (CAVs) get too close to each other which rarely occurs. In the simulation of our scheme, each time a HSU needs a HO, the new channel for this vehicle is randomly (with uniform distribution) selected from the list of all available channels. As we have a random selection of channels, random movement of vehicles, and very low HO rate in the proposed scheme, the output result for one iteration of our scheme will not be smooth. Therefore, we use the Monte-Carlo method with 500 iterations for each point and average the number of HOs to get the final result. This causes fractional numbers of HOs in our graph. These fractional numbers of HOs are more noticeable for lower number of users, since in the VFR scheme the HO occurrence rate is very low and accordingly the average will be just a fractional number less than even one (e.g., the first point of the red graph in Figure 14).

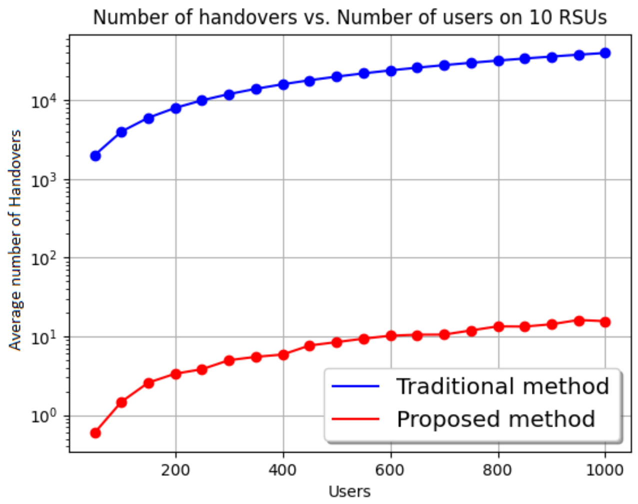

FIGURE 13. Number of handovers in 10 RSUs for different number of vehicles.

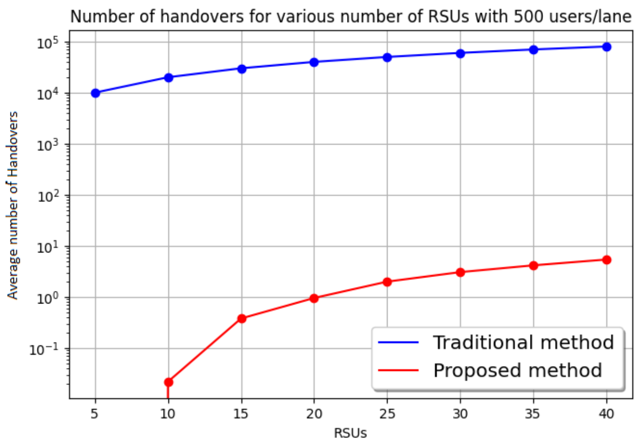

FIGURE 14. Number of handovers for 400 users for different number of RSUs.

In Figure 13, the horizontal axis shows the number of simulated vehicles in each lane. Therefore, the total number of vehicles on the road is four times the number on X-axis. This figure shows a remarkable reduction of the number of HOs in our proposed method compared with the traditional cellular network without any considerable processing cost or any change in the network infrastructure. Moreover, similar to the traditional cellular networks, the number of HOs in our proposed VFR scheme increases linearly with the number of users on the road. A comparison of the number of HOs between the two simulated schemes in Figure 13 reveals a consistent reduction in HO rate of over 99% and up to 99.96% in our proposed method (VFR scheme) for any number of users.

Figure 14 shows the number of HOs for different number of RSUs while the total number of users on each lane is fixed. In this figure, we consider 500 CAVs in each lane and we use a Monte-Carlo algorithm with 500 iterations, while the rest of the simulation parameters are the same as Figure 13. The horizontal axis shows the number of RSUs that we considered and the vertical axis shows the number of HOs happened at each equivalent number of RSUs for 500 CAVs passed through each of the four lanes. Since there is a big difference between the number of HOs for each number of users, we used logarithmic scale on the y-axis. This figure shows that the number of HOs in both methods linearly increases with the number of RSUs. However, our proposed VFR scheme has over 99% HO reduction compared to the traditional channel allocation scheme. In Figure 14, the number of HOs for our proposed method at 5 RSUs is zero (or negative infinity in logarithm) which explains the disconnection between the 5 and 10 RSUs for red line. Since the number of HOs for 10 RSUs were zero or very small in most of the iterations (500 Monte-Carlo iterations), their average is slightly less than its actual value. By increasing number of Monte-Carlo iterations, the average HO rate will get closer to the expected value in low number of RSUs and the graph will increase smoothly. However, the number of HOs for 15 or more RSUs are the expected value and will not change by the increasing the number of Monte-Carlo iterations.

XI. CONCLUSION

In this paper, we proposed a new Vehicular Frequency Reuse (VFR) scheme that improves cellular network performance for high-speed 5G users including CAVs, human driven cars, and trains. Our scheme is a user-centric channel allocation scheme for 5G terrestrial high-speed users serviced by the 5G-NR small-cells with FR2 (mm-Wave) bands. To establish the VFR scheme in 5G network, we designed a new mobility management function with a novel cell reselection procedure for high-speed users in RRC_Connected state while using the VFR scheme. The VFR scheme is completely compatible with the 5G and works with the existing network infrastructure without any hardware changes. The proposed mobility management function that applies the VFR scheme along with the traditional channel allocation scheme, can be easily added to any gNodeBs (NG-RAN nodes) with only a software patch update in network nodes. We also introduced a Distance-Threshold (DT) metric to calculate the minimum allowed distance between two CAVs using the same channel. Another metric, named the Velocity-Threshold (VT), is proposed and uses the K-Means clustering algorithm to calculate thresholds to separate low-speed and high-speed users in each direction of a road by their reported velocities. Hence, high-speed users are controlled by the proposed user-centric VFR scheme while low-speed users are managed by the traditional cell-centric channel allocation scheme. The simulation results show that the proposed scheme, reduces the number of handovers for high-speed CAVs by over 99% compared with the traditional scheme.

APPENDIX
ABBREVIATIONS

Table of the frequently used abbreviations in alphabetical order.

Abbr.	**Definition**
3GPP	3rd Generation Partnership Project.
5G	Fifth Generation.
5G-NR	5G-New Radio.
5GC	5G Core Network.
AV	Autonomous Vehicle.
CAV	Connected Autonomous Vehicle.
CID	Cell Identifier.
CU	Central Unit.
DAPS	Dual Active Protocol Stack.
DT	Distance-Threshold.
DU	Distributed Unit.
FR1	Frequency Range 1 (Below 6GHz).
FR2	Frequency Range 2 (above 24GHz).
gNB	Next Generation Node B (gNodeB).
HIT	Handover Interruption Time.
HO	Handover.
HSCH	High-Speed user's Channel.
HST	High-Speed Train.
HSU	High-Speed User.
IAB	Integrated access and backhaul.
ISD	Inter-Site Distance.
ITU	International Telecommunication Union.
ITU-T	ITU Telecomm. Standardization Sector.
LEO	Low Earth Orbit.
LOS	Line-of-Sight.
LSCH	Low-Speed user's Channel.
LSU	Low-Speed User.
LTE	Long Term Evolution.
MIMO	Multiple Input Multiple Output.
ML	Machine Learning.
MMF	Mobility Management Function.
mm-Wave	Millimetre Wave.
NG-RAN	Next Generation Radio Access Network.
NOMA	Non-Orthogonal Multiple Access.
NTN	Non-Terrestrial Network.
QoE	Quality of Experience.
QoS	Quality of Service.
RAN	Radio Access Network.
RAT	Radio Access Technology.
RRC	Radio Resource Control.
RSRP	Reference Signal Received Power.
RSRQ	Reference Signal Received Quality.
RSSI	Received Signal Strength Indicator.
RU	Radio Unit.
SDN	Software-Defined Networking.
SINR	Signal to Interference plus Noise Ratio.
UE	User Equipment.
UHPA	Uniform Hexagonal Planar Array.
V2N	Vehicle-to-Network.
V2X	Vehicle-to-Everything.
VANET	Vehicular Ad-oc Network.
VFR	Vehicular Frequency Reuse.
VT	Velocity-Threshold.

REFERENCES

[1] A. Cardon and M. Itmi, *New Autonomous Systems*, vol. 1. Hoboken, NJ, USA: Wiley, 2016.

[2] M. S. Elbamby, C. Perfecto, C.-F. Liu, J. Park, S. Samarakoon, X. Chen, and M. Bennis, "Wireless edge computing with latency and reliability guarantees," *Proc. IEEE*, vol. 107, no. 8, pp. 1717–1737, Aug. 2019.

[3] *System Architecture for the 5G System (5GS); Stage 2*, document TS 23.501, V17.6.0, Release 17, 3GPP, Sep. 2022, pp. 1–571.

[4] R. Atallah, C. Assi, and M. Khabbaz, "Deep reinforcement learning-based scheduling for roadside communication networks," in *Proc. 15th Int. Symp. Modeling Optim. Mobile, Ad Hoc, Wireless Netw. (WiOpt)*, May 2017, pp. 1–8.

[5] *Overall Description of Radio Access Network (RAN) Aspects for Vehicle-to-Everything (V2X) Based on LTE and NR*, document TR 37.985, V17.1.1, 3GPP, Release 17, Mar. 2022, pp. 1–38.

[6] *Base Station (BS) Radio Transmission and Reception*, document TS 38.104, V17.7.0, 3GPP, Release 17, Sep. 2022, pp. 1–359.

[7] R. Yu, J. Ding, X. Huang, M.-T. Zhou, S. Gjessing, and Y. Zhang, "Optimal resource sharing in 5G-enabled vehicular networks: A matrix game approach," *IEEE Trans. Veh. Technol.*, vol. 65, no. 10, pp. 7844–7856, Oct. 2016.

[8] M. Simsek, D. Zhang, D. Öhmann, M. Matthé, and G. Fettweis, "On the flexibility and autonomy of 5G wireless networks," *IEEE Access*, vol. 5, pp. 22823–22835, 2017.

[9] I. F. Akyildiz, S. Nie, S.-C. Lin, and M. Chandrasekaran, "5G roadmap: 10 key enabling technologies," *Comput. Netw.*, vol. 106, pp. 17–48, Sep. 2016.

[10] V. Kumar, S. Yadav, D. N. Sandeep, S. B. Dhok, R. K. Barik, and H. Dubey, "5G cellular: Concept, research work and enabling technologies," in *Advances in Data and Information Sciences* (Lecture Notes in Networks and Systems), vol. 39, M. Kolhe, M. Trivedi, S. Tiwari, and V. Singh, Eds. Singapore: Springer, 2019, doi: 10.1007/978-981-13-0277-0_27.

[11] I. Parvez, A. Rahmati, I. Guvenc, A. I. Sarwat, and H. Dai, "A survey on low latency towards 5G: RAN, core network and caching solutions," *IEEE Commun. Surveys Tuts.*, vol. 20, no. 4, pp. 3098–3130, 4th Quart., 2018.

[12] S. Tabbane, "Session 7: 5G networks and 3GPP release 15," Suva, Fiji, Tech. Rep., 2018. [Online]. Available: https://www.itu.int/en/ITU-D/Regional-Presence/AsiaPacific/SiteAssets/Pages/ITU-ASP-CoE-Training-on-/session7_5Gnetworks and 3GPP release 15.pdf

[13] *Radio Resource Control (RRC) Protocol Specification*, document TS 38.331, V17.2.0, 3GPP, Release 17, Sep. 2022, p. 1298.

[14] *Requirements for Support of Radio Resource Management*, document TS 38.133, V17.7.0, 3GPP, Release 17, Sep. 2022, pp. 1–5136.

[15] *NR and NG-RAN Overall Description; Stage 2*, document TS 38.300, V17.1.0, 3GPP, Release 17.1.0, Jun. 2022, pp. 1–209.

[16] *NG-RAN Architecture Description*, document TS 38.401, V17.1.1, 3GPP, Release 17, Jul. 2022, pp. 1–122.

[17] "Innovations in 5G backhaul technologies: IAB, HFC and fiber," 5G Amer., Washington, DC, USA, White Paper, 2020, pp. 1–62.

[18] *Study on New Radio Access Technology: Radio Access Architecture and Interfaces*, document TR 38.801, V14.0.0, 3GPP, Release 14, Mar. 2017, pp. 1–91.

[19] *Enhancement of 3GPP Support for V2X Scenarios; Stage 1*, document TS 22.186, V17.0.0, 3GPP, Release 17, Mar. 2022, pp. 1–18.

[20] *Study on Scenarios and Requirements for Next Generation Access Technologies*, document TR 38.913, 3GPP, V17.0.0, Release 17, Mar. 2022.

[21] S. A. Busari, M. A. Khan, K. M. S. Huq, S. Mumtaz, and J. Rodriguez, "Millimetre-wave massive MIMO for cellular vehicle-to-infrastructure communication," *IET Intell. Transp. Syst.*, vol. 13, no. 6, pp. 983–990, Jun. 2019.

[22] X. Wang, L. Wang, C. Cavdar, M. Tornatore, G. B. Figueiredo, H. S. Chung, H. H. Lee, S. Park, and B. Mukherjee, "Handover reduction in virtualized cloud radio access networks using TWDM-PON fronthaul," *J. Opt. Commun. Netw.*, vol. 8, no. 12, pp. B124–B134, Dec. 2016.

[23] *User Equipment (UE) Procedures in Idle Mode and RRC Inactive State*, 3GPP, Release 17, Sep. 2022, pp. 1–50.

[24] *Procedures for the 5G System (5GS); Stage 2*, document TS 23.502, V17.6.0, 3GPP, Release 17, Sep. 2022, p. 748.

[25] *3GPP Evolved Packet System (EPS); Evolved General Packet Radio Service (GPRS) Tunnelling Protocol for Control Plane (GTPv2-C); Stage 3*, document TS 29.274, V18.1.0, 3GPP, Release 18, Dec. 2022, pp. 1–417.

[26] J.-H. Choi and D.-J. Shin, "Generalized RACH-less handover for seamless mobility in 5G and beyond mobile networks," *IEEE Wireless Commun. Lett.*, vol. 8, no. 4, pp. 1264–1267, Aug. 2019.

[27] O. Ohlsson, P. Wallentin, and C.-G. Persson, "Reducing mobility interruption time in 5G networks," Ericsson, Apr. 2020. [Online]. Available: https://www.ericsson.com/en/blog/2020/4/reducing-mobility-interruption-time-5g-networks

[28] V. Yajnanarayana, H. Rydén, and L. Hévizi, "5G handover using reinforcement learning," in *Proc. IEEE 3rd 5G World Forum (5GWF)*, Sep. 2020, pp. 349–354.

[29] J. Baik, C. Lee, J. Jung, and J.-M. Chung, "5G mmWave multiple active protocol stack optimized deep learning handover," *IEEE Wireless Commun. Lett.*, vol. 11, no. 11, pp. 2265–2269, Nov. 2022.

[30] A. Çalhan and M. Cicioğlu, "Handover scheme for 5G small cell networks with non-orthogonal multiple access," *Comput. Netw.*, vol. 183, Dec. 2020, Art. no. 107601.

[31] L. P. Qian, Y. Wu, H. Zhou, and X. Shen, "Non-orthogonal multiple access vehicular small cell networks: Architecture and solution," *IEEE Netw.*, vol. 31, no. 4, pp. 15–21, Jul. 2017.

[32] G. Li and C. Lai, "Platoon handover authentication in 5G-V2X: IEEE CNS 20 poster," in *Proc. IEEE Conf. Commun. Netw. Secur. (CNS)*, Jun. 2020, pp. 1–2.

[33] N. Zohar, "Beyond 5G: Reducing the handover rate for high mobility communications," *J. Commun. Netw.*, vol. 24, no. 2, pp. 154–165, Apr. 2022.

[34] *Summary of Rel-17 Work Items*, document TR 21.917, V1.0.0, 3GPP, Release 17, Sep. 2022, pp. 1–165.

[35] E. Juan, M. Lauridsen, J. Wigard, and P. Mogensen, "Handover solutions for 5G low-earth orbit satellite networks," *IEEE Access*, vol. 10, pp. 93309–93325, 2022.

[36] V. Saritha, P. V. Krishna, S. Misra, and M. S. Obaidat, "Learning automata-based channel reservation scheme to enhance QoS in vehicular adhoc networks," in *Proc. IEEE Global Commun. Conf. (GLOBECOM)*, Dec. 2016, pp. 1–6.

[37] C. Lee, J. Jung, and J.-M. Chung, "Intelligent dual active protocol stack handover based on double DQN deep reinforcement learning for 5G mmWave networks," *IEEE Trans. Veh. Technol.*, vol. 71, no. 7, pp. 7572–7584, Jul. 2022.

[38] K. Zhou, C. Gong, N. Wu, and Z. Xu, "Distributed channel allocation and rate control for hybrid FSO/RF vehicular ad hoc networks," *J. Opt. Commun. Netw.*, vol. 9, no. 8, pp. 669–681, Aug. 2017.

[39] X. Zhao, X. Zhang, and Y. Li, "A hierarchical resource allocation scheme based on Nash bargaining game in VANET," *Information*, vol. 10, no. 6, pp. 1–196, Jun. 2019.

[40] T. Zhao, S. Lu, W. Yan, and X. Li, "A road based multi-channel assignment method for VANET," in *Proc. Int. Conf. Comput., Netw. Commun. (ICNC)*, Jan. 2013, pp. 61–65.

[41] *Xn Application Protocol (XnAP)*, document TS 38.423, V17.2.0, 3GPP, Release 17, Sep. 2022, p. 614.

[42] R. Krajewski, J. Bock, L. Kloeker, and L. Eckstein, "The highD dataset: A drone dataset of naturalistic vehicle trajectories on German highways for validation of highly automated driving systems," in *Proc. 21st Int. Conf. Intell. Transp. Syst. (ITSC)*, Nov. 2018, pp. 2118–2125.

[43] R. Chow, J. Mah, R. Duckworth, B. Bielkiewicz, J. Aoro, G. Dunn, D. Ekkelenkamp, B. Latte, H. Putz, and P. Shaflik, "Highway lighting guide," Alberta Transp., AB, Canada, Aug. 2003. [Online]. Available: https://open.alberta.ca/publications/highway-lighting-guide

[44] W. Tan, S. D. Assimonis, M. Matthaiou, Y. Han, X. Li, and S. Jin, "Analysis of different planar antenna arrays for mmWave massive MIMO systems," in *Proc. IEEE 85th Veh. Technol. Conf. (VTC Spring)*, Jun. 2017, pp. 1–5.

[45] M. Raeisi and A. B. Sesay, "A distance metric for uneven clusters of unsupervised K-means clustering algorithm," *IEEE Access*, vol. 10, pp. 86286–86297, 2022.

[46] S. Chandra and A. K. Bharti, "Speed distribution curves for pedestrians during walking and crossing," *Proc.-Social Behav. Sci.*, vol. 104, pp. 660–667, Dec. 2013.